DOI: 10.1534/genetics.104.032334

Mutations That Rescue the Paralysis of *Caenorhabditis elegans ric-8* (Synembryn) Mutants Activate the $G\alpha_s$ Pathway and Define a Third Major Branch of the Synaptic Signaling Network

Michael A. Schade,[1] Nicole K. Reynolds,[1] Claudia M. Dollins[2] and Kenneth G. Miller[3]

Program in Molecular, Cell and Developmental Biology, Oklahoma Medical Research Foundation, Oklahoma City, Oklahoma 73104

Manuscript received June 15, 2004
Accepted for publication October 12, 2004

ABSTRACT

To identify hypothesized missing components of the synaptic $G\alpha_o$-$G\alpha_q$ signaling network, which tightly regulates neurotransmitter release, we undertook two large forward genetic screens in the model organism *C. elegans* and focused first on mutations that strongly rescue the paralysis of *ric-8(md303)* reduction-of-function mutants, previously shown to be defective in $G\alpha_q$ pathway activation. Through high-resolution mapping followed by sequence analysis, we show that these mutations affect four genes. Two activate the $G\alpha_q$ pathway through gain-of-function mutations in $G\alpha_q$; however, all of the remaining mutations activate components of the $G\alpha_s$ pathway, including $G\alpha_s$, adenylyl cyclase, and protein kinase A. Pharmacological assays suggest that the $G\alpha_s$ pathway-activating mutations increase steady-state neurotransmitter release, and the strongly impaired neurotransmitter release of *ric-8(md303)* mutants is rescued to greater than wild-type levels by the strongest $G\alpha_s$ pathway activating mutations. Using transgene induction studies, we show that activating the $G\alpha_s$ pathway in adult animals rapidly induces hyperactive locomotion and rapidly rescues the paralysis of the *ric-8* mutant. Using cell-specific promoters we show that neuronal, but not muscle, $G\alpha_s$ pathway activation is sufficient to rescue *ric-8(md303)*'s paralysis. Our results appear to link RIC-8 (synembryn) and a third major Gα pathway, the $G\alpha_s$ pathway, with the previously discovered $G\alpha_o$ and $G\alpha_q$ pathways of the synaptic signaling network.

INTENSIVE research over the past 15 years has yielded a molecular description of the core machinery that drives synaptic vesicle fusion and neurotransmitter release (Lin and Scheller 2000; Rizo and Sudhof 2002). Although important questions remain, a major challenge now becomes to define and to understand the logic of the network of signal transduction pathways that regulates neurotransmitter release, because these pathways are likely to serve as key substrates for behavioral modification, learning, and memory.

The available evidence suggests that as many as three major classes of Gα signaling proteins could be involved in regulating different aspects of neurotransmitter release: $G\alpha_q$, $G\alpha_{o/i}$, and $G\alpha_s$. Biochemical studies have revealed that the binding of neurotransmitter to receptors coupled to these G proteins causes the receptors to act as guanine-nucleotide exchange factors (GEFs) that put the Gα protein in the GTP-bound activated state and facilitate its dissociation from the βγ subunits of the G protein (Hepler and Gillman 1992; Neer 1995; Bourne 1997). Our knowledge of how these three major Gα pathways affect neurotransmitter release is a mixture of single pathway studies and other intriguing, but poorly understood, observations. For example, we know that the $G\alpha_q$ pathway produces, among other possible effectors, the small molecule diacylglycerol (DAG; Singer *et al.* 1997). Although the effects on neurotransmitter release of knocking out the $G\alpha_q$ pathway have not been investigated, experiments using phorbol esters (molecular analogs of DAG) suggest that activating the $G\alpha_q$ pathway can strongly potentiate evoked neurotransmitter release and even stimulate spontaneous release (Malenka *et al.* 1986; Parfitt and Madison 1993; Stevens and Sullivan 1998; Hori *et al.* 1999; Waters and Smith 2000). Proteins of the $G\alpha_{o/i}$ family arouse interest because of their puzzling localization on synaptic vesicles (Ngsee *et al.* 1990; Aronin and DiFiglia 1992; Ahnert-Hilger *et al.* 1994) and because they are found at remarkably high concentrations in brain (Sternweis and Robishaw 1984). The third pathway, controlled by $G\alpha_s$, clearly plays an important role in learning and memory and in the synaptic facilitation paradigms thought to represent physiological correlates for some forms of learning and memory (Davis *et al.* 1995; Kandel and Pittenger 1999; Kandel 2001).

The logic behind how these three pathways interact with each other, if indeed they do, has largely eluded researchers. Do the pathways intersect/converge, or do

[1]These authors contributed equally to this work.

[2]*Present address:* Molecular Genetics and Microbiology, Duke University, 268 CARL Bldg., Research Dr., Box 3054, Durham, NC 27710.

[3]*Corresponding author:* Program in Molecular, Cell and Developmental Biology, Oklahoma Medical Research Foundation, 825 NE 13th St., Oklahoma City, OK 73104.
E-mail: millerk@omrf.ouhsc.edu

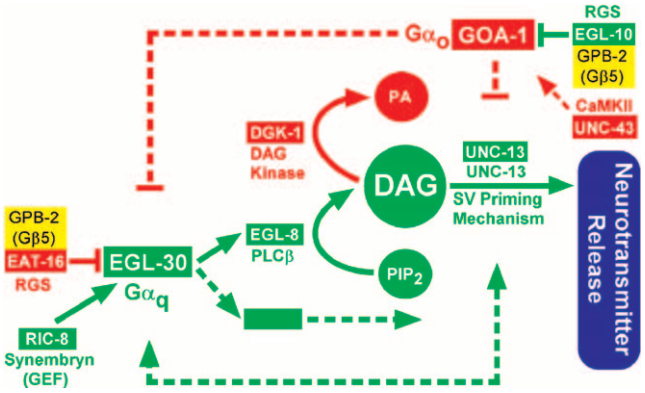

FIGURE 1.—Pathway model of the $G\alpha_o$-$G\alpha_q$ signaling network as inferred from *C. elegans* genetic studies. Solid lines indicate that direct interactions are known or likely, while dashed lines and/or large gaps between line endpoints and downstream effectors indicate predicted interactions or missing components. Proteins that positively regulate neurotransmitter release are shown in green. Reducing green protein function results in aldicarb resistance, paralysis or decreased locomotion, decreased egg laying, and, in some cases, paralytic larval arrest. Proteins that inhibit neurotransmitter release are shown in red blocks. Reducing red protein function results in aldicarb hypersensitivity and increased rates of locomotion and egg laying. The bottom green dashed lines represent hypothetical components (searched for using the genetic screens herein) that could positively regulate the EGL-30 ($G\alpha_q$) pathway to establish or maintain synapse activation. This model is based on the following studies: MARUYAMA and BRENNER (1991), MENDEL *et al.* (1995), SEGALAT *et al.* (1995), BRUNDAGE *et al.* (1996), KOELLE and HORVITZ (1996), HAJDU-CRONIN *et al.* (1999), LACKNER *et al.* (1999), MILLER *et al.* (1999, 2000), NURRISH *et al.* (1999), RICHMOND *et al.* (1999, 2001), ROBATZEK and THOMAS (2000), CHASE *et al.* (2001), ROBATZEK *et al.* (2001), VAN DER LINDEN *et al.* (2001), BASTIANI *et al.* (2003), and TALL *et al.* (2003).

they represent independent parallel pathways? What are the key downstream effectors that mediate the interactions of each pathway with the neurotransmitter release machinery? Are the pathways active only in response to receptor stimulation, or can they be kept active independently of continued receptor input? Finally, what determines when and where the pathways are active to ultimately produce, or allow, a coherent, coordinated behavior?

Genetic studies of the *Caenorhabditis elegans* EGL-30 ($G\alpha_q$) pathway have begun to shed light on some of these questions by revealing a large network of proteins that regulates neurotransmitter release (Figure 1). As in vertebrates, $G\alpha_q$'s action in the *C. elegans* nervous system appears to be mediated by phospholipase Cβ (EGL-8), although the *C. elegans* studies also point to one or more unidentified $G\alpha_q$ effectors (LACKNER *et al.* 1999; MILLER *et al.* 1999; BASTIANI *et al.* 2003). According to the model, EGL-8 (PLCβ) makes the small molecule DAG, which is involved in activating the synaptic vesicle priming mechanism by binding to, among other possible targets, the C1 domain of UNC-13 (MARUYAMA and BRENNER 1991), which is a large, conserved protein that interacts with the synaptic vesicle fusion machinery (BETZ *et al.* 1997; SASSA *et al.* 1999) and which is required for synaptic vesicle priming (ARAVAMUDAN *et al.* 1999; AUGUSTIN *et al.* 1999; RICHMOND *et al.* 1999; RICHMOND *et al.* 2001). *C. elegans* researchers can identify proteins involved in EGL-30 ($G\alpha_q$) signaling through genetic screens centered around easily recognizable phenotypes that affect locomotion, egg laying, and growth on aldicarb. Loss-of-function mutations in positive regulators of neurotransmitter release (the green proteins in Figure 1) tend to cause paralysis, decreased egg laying, and resistance to aldicarb, while loss-of-function mutations in negative regulators (the red proteins in Figure 1) tend to cause hyperactive locomotion and egg laying and hypersensitivity to aldicarb. In recent years, genetic screens centered on these phenotypes, as well as related suppressor screens, have begun to uncover a large network of proteins. This network includes another major Gα protein, GOA-1 ($G\alpha_o$), which negatively regulates the EGL-30 ($G\alpha_q$) pathway by one or more unknown mechanisms, a DAG kinase that antagonizes the EGL-30 pathway, and two RGS proteins that negatively regulate each Gα protein (see Figure 1 and references in its legend).

While many aspects of the model in Figure 1 are well supported, other connections are poorly understood, as represented by the dashed lines in the model. In addition, the model includes several mechanisms for negatively regulating the $G\alpha_q$ pathway, but it seems reasonable to expect that synapses might have one or more mechanisms for positively regulating the $G\alpha_q$ pathway, perhaps even in the absence of continuous receptor stimulation. Such a need might arise, for instance, if a synapse needed to be kept in an active state for an extended period of time. One protein that appears required for proper activation of the EGL-30 ($G\alpha_q$) pathway is RIC-8 (synembryn), originally identified in *C. elegans* as a novel, conserved protein that functions upstream of EGL-30 ($G\alpha_q$) (MILLER *et al.* 2000) and recently revealed by biochemical studies to be a GEF that helps monomeric Gα subunits (including, but not limited to, $G\alpha_q$) to attain the GTP-bound activated state independently of receptor stimulation (TALL *et al.* 2003; Figure 1). However, given the central importance of the core $G\alpha_q$ pathway with respect to neurotransmitter release (REYNOLDS *et al.* 2005, accompanying article in this issue), we hypothesized that there could be other components, in addition to RIC-8, that positively regulate, or otherwise impinge upon, the EGL-30 ($G\alpha_q$) pathway (Figure 1).

To identify some of these hypothetical missing components, and others alluded to above, we undertook two large forward genetic screens and focused first on mutations that strongly suppress the paralysis associated with reduced RIC-8 function. Our results appear to link RIC-8 (synembryn) and a third major Gα pathway, the

$G\alpha_s$ pathway, with the previously discovered $G\alpha_o$-$G\alpha_q$ signaling network. Together with the accompanying study (Reynolds *et al.* 2005), these results suggest that three highly conserved Gα signaling pathways form the synaptic signaling network, an integrated molecular circuit that is likely to be a major substrate for behavioral modification, learning, and memory.

MATERIALS AND METHODS

Worm culture and observation: Twenty-four-well culture plates (Evergreen 222804401F) were prepared in sets of 80 or 120 using a plate-dispensing machine to dispense 2.8 ml (for genetic screening plates) or 2.3 ml (for integration plates) into each well. Plates were cured 3 days at room temperature before seeding each well with 10 μl of OP-50 culture using a repeat pipetter with a sterile tip. Seeded plates were dried for 1 hr in a 37° room with the lids off before returning to room temperature for 4 more days, stacked lid side up. Plates were then wrapped in plastic wrap and stored at room temperature or 4°. All culture media was made with Sigma (St. Louis) A-7002 agar. All other worm culture was based on previously described methods (Brenner 1974). Worms were observed and manipulated using Olympus SZX-12 stereomicroscopes equipped with ×1.2, 0.13 numerical aperture plan apochromatic objectives. Unless otherwise specified, wild-type worms were *C. elegans* variety Bristol, strain N2. *acy-1(pk1279)* was maintained over the closely linked mutation *dpy-17(e164)* as the strain NL1999, which was kindly provided by Celine Moorman and Ron Plasterk.

Genetic screens: All but one of the mutants described in this article were isolated in the genetic screens described below. A clonal screen for mutants with hyperactive locomotion was performed in weekly cycles by plating 2000 mature adult F_1 progeny of ethyl methanesulfonate (EMS)-mutagenized N2 hermaphrodites on individual wells of 24-well culture plates. Plates were loaded in the afternoon and incubated overnight at 14°, which allowed each F_1 to lay an average of ~40 eggs. To prevent the small food supply in each well from being exhausted before potentially slow-growing mutant F_2's fully matured, the F_1's were picked from each well and killed after the overnight incubation at 14°. The F_2 progeny on the plate were then allowed to mature to adulthood by incubating 23 hr at 14° followed by 72 hr at 20°. At this point the plates were screened, and wells perceived to contain hyperactive mutants were noted. From these wells, three to five candidate hyperactive mutants were cloned to individual streak plates and incubated 5 days at 20° to produce populations of animals. A plate containing a population judged to be homozygous for a hyperactive mutation was then scored for various hyperactive behaviors and characteristics and then used to produce a working stock and frozen culture.

Similarly, a clonal screen for mutations that suppress the nearly paralyzed phenotype of *ric-8(md303)* mutants was performed in weekly cycles by plating 2000 mature adult F_1 progeny of EMS-mutagenized *ric-8(md303)* hermaphrodites on 24-well culture plates. The plating methods were the same as described for the N2 screen, except that the F_1 populations used for plating were allowed to mature at 14°, since *ric-8(md303)* produces larger broods at this temperature. The plated F_1's were incubated overnight at 14° followed by 4 days at 20° before screening. Wells were screened as described for the N2 hyperactive screen, except that the plates were regularly picked up and dropped on the microscope stage to provide a stimulus for movement. Unstarved *ric-8(md303)* single mutants only rarely show movement in response to this stimulus, whereas *ric-8(md303)* animals containing a strong suppressor mutation will move well, often even in the absence of plate dropping.

Screens were performed as described above, in weekly cycles, alternating between 3 successive cycles of each screen, for 16 cycles for the *ric-8* suppressor screen and 12 cycles for the N2 hyperactive screen. We estimate that each cycle screened 3000 mutagenized genomes for a total of 48,000 mutagenized genomes for the *ric-8* suppressor screen and 36,000 for the N2 hyperactive screen. The *md1756* mutation was isolated in a previously described smaller genetic screen for suppressors of *ric-8(md303)* (Miller *et al.* 1999).

Complementation tests and outcrossing: When analyzing new mutants isolated in the hyperactive mutant screen, mutants that strongly resembled loss-of-function mutations in one of the known genes of *goa-1*, *dgk-1*, *eat-16*, or *gpb-2* were immediately complement tested with a known mutant in the suspected gene, using standard methods. Mutants not corresponding to the known genes were outcrossed four times by crossing heterozygous males with *dpy-5(e61)* hermaphrodites and then reisolating the mutation in the F_2 generation and repeating this procedure once.

Mutants isolated in the *ric-8(md303)* suppressor screen were first analyzed by crossing N2 males to *ric-8(md303); sup-x* double-mutant hermaphrodites and then isolating putative homozygous *sup-x* single mutants in the F_2 generation. One-time outcrossed suppressor mutants that were X-linked and resembled *dgk-1* mutants were immediately complement tested against *dgk-1*. All other one-time outcrossed suppressor mutants were crossed back into a *ric-8(md303)* background to test suppression by crossing *sup-x*/+ males to *ric-8(md303)* hermaphrodites and reisolating three-time outcrossed versions of both the *sup-x* single mutant and the ric-*8(md303); sup-x* double mutant in the F_2 generation. This cross was then repeated to produce five-time outcrossed versions of the *sup-x* single and the *ric-8(md303); sup-x* double mutants.

The dominant mutation *acy-1(md1756)* was outcrossed in a *ric-8(md303)* background by crossing *md1756; md303* males to *md303* hermaphrodites. Suppressed male progeny of this cross (genotype md1756/+*; md303/md303*) were then crossed again to *ric-8(md303)*, and this process was repeated two times. Suppressed virgin hermaphrodite progeny from the final cross were then allowed to self-fertilize, and candidate homozygous four-time outcrossed *md1756; md303* double mutants were isolated and confirmed by the absence of *md303* single mutants in the next generation. *md1756* single mutants were isolated after the mutation was mapped (see below) by first placing *md1756* over the balancer *qC1* to facilitate identification of *md1756* homozygotes.

The *egl-30(ce263)* mutation was lethal in a wild-type background or as the *trans*-heterozygote *ce263/+; md303/+*. This mutation was therefore outcrossed by crossing *md303/+* males to *ce263; md303* hermaphrodites and reisolating putative *ce263; md303* double mutants in the F_2 generation. Putative double mutants were tested for homozygosity by allowing them to self-fertilize and then checking for the absence of *ric-8(md303)* single mutants among the self-progeny.

Mapping and sequencing mutations: All mutations were mapped entirely with respect to single nucleotide polymorphisms (SNPs) using the CB4856 SNP mapping strain (Table 1). Most of the mutations were mapped by crossing CB4856 males to homozygous mutant hermaphrodites. Virgin F_1 hermaphrodite progeny of this cross were then cloned to individual culture plates and allowed to self-fertilize. Candidate homozygous mutants were then reisolated from the resulting F_2 population and cloned to individual streak plates. The progeny of these animals were then checked for homozygosity (absence of wild-type animals), and, upon starvation, we

TABLE 1

SNPs used to fine map synaptic signaling network mutations

Linkage group	Allele	Genetic position[a]	Clone location on clone	Method of ID[b]	Enzyme	N2 products (bp)	CB4856 products (bp)
I	*ceP27*	−21.50	ZC123-21628	Snip-SNP	*Ssp*I	347	195/152
I	*ceP28*	−17.64	Y48G8AR-11223	Snip-SNP	*Apo*I	306	193/113
I	*ceP32*	−19.96	C45G6-19957	Snip-SNP	*Bsi*EI	329	188/141
I	*ceP75*	−13.85	Y71G12B-85969	Snip-SNP	*Bsa*HI	735	446/289
I	*ceP76*	−12.50	Y71G12A-29112	Snip-SNP	*Ssp*I	597	374/223
III	*ceP35*	−3.44	F25F2-15611	Snip-SNP	*Dde*I	394	231/163
III	*ceP39*	−2.14	Y54H5A-20087	Snip-SNP	*Tsp*RI	350	220/130
III	*ceP42*	−2.56	F26A1-7094	Seq-SNP	NA	NA	NA
X	*ceP34*	−3.93	Y23B4A-12491	Snip-SNP	*Hpy*188I	370	232/138
X	*ceP43*	−3.32	T13C5-12745	Snip-SNP	*Rsa*I	355	239/116
X	*ceP45*	−3.77	F22F4-6421	Seq-SNP	NA	NA	NA

Listed are the SNP markers used to fine map the mutations described in Figure 2 of this article. SNP assays were designed as described above in the supplemental SNP mapping protocol at http://www.genetics.org/supplemental/, using data derived from Wicks *et al.* (2001) and the *C. elegans* SNP website (http://genome.wustl.edu/projects/celegans/index.php?snp=1). The unique allele numbers assigned to each SNP used in this article are not meant to be official names of these SNPs, since they were all previously discovered (Wicks *et al.* 2001) and may now have other names.

[a] Extrapolated genetic position as given by WormBase Freeze WS100 (http://www.wormbase.org).

[b] Snip-SNP, a SNP identified by restriction digest; Seq-SNP, a SNP identified by sequencing.

checked the homozygous cultures for various CB4856 SNPs using the methods described below.

acy-1(md1756) was mapped by its suppressor activity in a *ric-8 (md303)* background by crossing *md1756; ric-8(md303)* males to a strain of *ric-8(md303)* that had been outcrossed 12 times into a CB4856 background. Virgin cross progeny were cloned to individual culture plates and putative homozygous *md1756; ric-8(md303)* double mutants were reisolated from the progeny of these animals and cloned to individual plates. Homozygosity was confirmed after one to two generations and the plates were allowed to starve out and processed as described below.

egl-30(ce263) was mapped by crossing CB4856 males to *ric-8 (md303)* (12 times outcrossed into CB4856) and crossing the resulting *md303/+* (CB4856) males to *ce263; md303* hermaphrodites. Only cross progeny homozygous for *md303* will survive this cross. Putative homozygous *ce263; md303* double mutants were then reisolated in the following generation, confirmed in the generation after this, and homozygous mutant cultures were allowed to starve out and processed as described below.

To map a mutation at high resolution, we typically isolated ~300–400 F_2 homozygous mutant progeny that had been crossed through the mapping strain and let their cultures go to starvation on individual culture plates before processing as described below.

Once a mutation had been mapped to an interval of <250 kb, we amplified candidate genes from mutant lysates and sequenced the coding exons and intron/exon boundaries as described (Miller *et al.* 2000).

Identification of cultures containing specific CB4856 SNPs: Starved cultures of homozygous mutants that had been passed through the CB4856 mapping strain were harvested and lysed in preparation for PCR by rinsing with 500 μl ddH_2O and by recovering 100 μl of the worm suspension. Suspensions were added to a 96- × 650-μl deep-well block (Marsh Bio Products, Rochester, NY). An equal volume (100 μl) of lysis buffer (50 mm KCl; 10 mm Tris-HCl, pH 8.2; 2.5 mm MgCl2; 0.45% Tween-20; 0.5 mg/ml gelatin; 200 μg/ml proteinase K) was added to each well. The block was sealed with a flexible mat lid (Marsh Bio Products) and placed at −85° for at least 1 hr and then double wrapped in plastic wrap and put in a hybridization oven (Bellco) at 65° for 4 hr. The plate was vortexed for ~30 sec after 1 hr at 65° and again at the end of the incubation period. To inactivate the proteinase K, the 96-well blocks were incubated in a Bellco hybridization oven at 95° for 30 min and then spun 5 min at 800 rpm to pellet insoluble debris. Control lysates (usually CB4856, prepared in a separate block) were usually added to selected wells left empty until this point. Blocks were stored for up to 1 month at 4° (double wrapped in plastic wrap) or frozen for longer storage.

Designing SNP assays: Using the *C. elegans* SNP database (http://genome.wustl.edu/projects/celegans/index.php?snp=1) we sought snip-SNPs in the regions of interest that could be identified by a restriction enzyme that cuts the SNP site in CB4856, but not in N2, and for which other sites cut by that enzyme (in both CB4856 and N2) are not closer than 90–100 bp from the unique SNP site. Primers were designed to be centered around the SNP such that, after cutting, the N2 SNP-containing fragment is ~400–750 bp in size and the CB4856 SNP-containing fragment is ~100 bp smaller.

SNP analysis: To identify which wells in a 96-well block of mutant lysates contain a specific snip-SNP, we dispensed 25 μl of a PCR master mix to the wells of a 96-well PCR plate. Each 25-μl reaction consists of 2.5 μl of 10× PCR buffer, 1 μl of a 10 pmol/μl stock of each primer, 2 μl of a dNTP stock (stock of 2.5 mm each dNTP), 2 μl of 30% sucrose, 1 μl of 0.1% cresol red, 15.4 μl of ddH_2O, and 0.122 μl of a 5 units/μl stock of Taq polymerase (Wicks *et al.* 2001). A 96-pin plastic replicator (Incyte Genomics ATD-5000) was then inserted into the 96-well block containing the mutant lysates. We noted that the PCR reactions worked significantly better if the 96-well block of mutant lysates was spun 3 min at 800 rpm within 5 min of replicating the lysates. The 96-well PCR plate containing the master mix was then placed, without its lid in place, in a thermal cycler [MJ Research (Watertown, MA) DNA engine] paused at the denaturation step of the first cycle. The 96-pin replicator was then withdrawn from the lysate block and immediately inserted in the PCR plate, swished briefly, and

withdrawn, dragging the spikes along the sides of each well. The PCR plate was then sealed with Microseal A film (MJ Research) using a roller to seal all regions of the plate. The PCR program was then resumed, and the reactions were PCR'ed for 35 cycles of 94° for 40 sec, 57° for 40 sec, and 72° for 40 sec, followed by 72° for 5 min. During thermal cycling, a restriction enzyme master mix was assembled, consisting of 3.5 μl of 10× buffer, 3.5 μl of 10 mg/ml bovine serum albumin, 1 μl of 30% sucrose, 0.5 μl of 0.1% cresol red, 4–5 units of enzyme, and ddH_2O to bring to 10 μl/reaction (Wicks *et al.* 2001). After thermal cycling, 10 μl of the restriction master mix was dispensed to each well followed by incubation at the optimal digest temperature for 2 hr. Products were resolved by loading 12 μl of each reaction on a 2% agarose 100-lane gel (Owl Centipede gel system with 2- × 50-well combs) with ethidium bromide (0.5 μg/ ml) included in the gel and buffer. Gels were run for 45 min at 140 V, and lanes containing CB4856 products were noted.

To test multiple snip-SNPs in parallel (*e.g.*, one snip-SNP from each chromosome), a PCR master mix was first prepared without primers and then divided equally into batches of 24 reactions before adding primers specific for each snip-SNP to be tested. The mixes were then dispensed to a PCR plate in sets of 24 and processed from there as described above. Similarly, restriction enzyme master mixes were first assembled without 10× buffer or enzyme and then divided into batches of 24 reactions before adding buffer and enzyme specific for each snip-SNP. In this way, a 96-well block that is only partially full (with at least 24 samples) can be used to test multiple SNPs.

To test specific lysates for SNPs by sequencing, we assembled, in individual 200-μl PCR tubes, 100-μl reactions with the same components as above, except we included no sucrose or cresol red, and 0.5 μl of sample lysate was added directly to each reaction. If the SNP had not been previously confirmed, CB4856 control lysates were PCR'ed in parallel. Reaction products were purified using the Wizard PCR Prep (Promega, Madison, WI) and submitted for sequence analysis using an appropriate primer.

Long PCR products and plasmids: All long PCR products were produced via Expand 20 kb+ (Roche) amplification of purified N2 genomic DNA, according to the manufacturer's instructions. The 12.4-kb *kin-2* gene rescuing PCR product KG370/371 includes ~5 kb of native *kin-2* upstream sequence as well as the *kin-2* gene and its putative 3′ control region. The pAC2 plasmid was kindly provided by Mike Nonet and contains the P260S gain-of-function mutation in the *acy-1* gene driven by the *acy-1* native promoter. To construct KG#81 [*myo-3::acy-1(gf)* cDNA], we applied reverse transcriptase to purified *C. elegans* mRNA and synthesized the 1155-bp 5′ part of the *acy-1* cDNA. This fragment was then fused to the partial cDNA clone yk35d9, using an internal *Sph*I site and a 5′ site that had been engineered into the 5′ primer. QuikChange mutagenesis was used to introduce the P260S gain-of-function mutation by changing a CCT to a TCT at nucleotide 778 from the start of the coding region. The 3.8-kb *acy-1* coding region was then amplified using Pfu ultra polymerase and primers engineered with restriction sites and cloned into *Age*I/*Xho*I-cut pPD96.52, a *C. elegans* muscle expression vector. The final construct was sequenced and a clone was chosen that contained no additional mutations. To make KG#83 [*rab-3::acy-1(gf)* cDNA], we used *Age*I/*Xho*I to cut out the 3800-bp *acy-1*(P260S) cDNA from KG#81 and cloned this fragment into like-digested KG#59, which is identical to pPD96.52 except that the *myo-3* promoter has been replaced with the 1.2-kb *rab-3* neuronal-specific promoter.

Production of transgenes: Transgenic strains bearing extrachromosomal arrays were produced by the method of Mello *et al.* (1991). pBluescript carrier DNA was used, if necessary, to bring the final concentration of DNA in the injection mixture to 175 ng/μl. *ceEX1* [*kin-2::kin-2* gene] was produced by injecting *kin-2(ce179)* mutants with the KG370/371 PCR product at 20 ng/μl, along with the marker plasmid pPD-118.20 [*myo-3::GFP*]. *ceEx49* [*acy-1::acy-1 (gf)* gene] was produced by injecting *pha-1(e2123)* animals with pAC2 at 2 ng/μl along with the *pha-1*(+) rescuing plasmid pBx (70 ng/μl). *ceIs6* [*myo-3::acy-1(gf)* cDNA] and *ceIs11* [*rab-3::acy-1(gf)* cDNA] were produced by injecting *pha-1(e2123)* animals with KG#81 (10 ng/μl) and KG#83 (10 ng/μl), respectively, along with the *pha-1*(+) cotransformation marker plasmid pBx, and then integrating the resulting transgenes. To integrate the transgenes, we irradiated growing cultures with 4200 rad of Cs-137 gamma irradiation, then picked four L4-stage animals to each of 12 culture plates and grew them 6 days at 25° to let the cultures starve. A chunk of media from each starved culture was then transferred to a fresh plate and grown 2 days at 25°. From each of the 12 plates, 24 adult animals were picked to wells of solid media on a 24-well plate (288 wells total) and grown 1 day at 25°. The adults were picked off and the plates were incubated 1 day at 25° to allow the eggs to hatch. Cultures were screened for 100% transmission of the temperature-sensitive embryonic-lethal *pha-1* marker by identifying wells that contained no unhatched eggs.

RNAi: For *kin-2* RNAi, the entire 1131-bp *kin-2* coding region was amplified by PCR, cloned into the L4440 RNAi vector, and transferred into the HT115(DE3) expression strain. After inducing expression of the double-stranded RNA, the *kin-2* RNAi expression strain was fed to wild-type animals and their progeny (Kamath *et al.* 2001; Timmons *et al.* 2001).

Double-mutant strain construction and verification: Unless otherwise specified, double mutants were constructed using standard genetic methods without additional marker mutations and were confirmed by crossing N2 males to the double mutant, cloning 12 L4 hermaphrodite cross progeny and confirming the presence of both mutant phenotypes and wild type among the progeny of each animal. Outcrossed versions of the *ric-8(md303); sup-x* double mutants isolated in this study were produced during outcrossing as described above. We constructed *gsa-1(ce81); acy-1(pk1279)* double mutants by crossing *ce81*/+ males to *pk1279/dpy-17(e164)* hermaphrodites. L4 progeny of this cross were then cloned and, from plates segregating both mutant phenotypes, 40 putative *pk1279/+; ce81* animals were cloned. From this group, plates found to be homozygous for *ce81* (no wild type) were tested for the presence of the *pk1279* mutation by PCR using primers flanking the *pk1279* deletion. *ce81* homozygous cultures found to carry *pk1279* were then expanded, and each culture was retested for the presence of the *pk1279* deletion. After collecting putative double-mutant larvae from these cultures for documentation and assays (see below), a portion of the population was used to confirm homozygosity of *pk1279* by duplicate reactions of double-amplification PCR using nested primers that are completely internal to the deletion and by comparing to wild-type positive control reactions amplified with the same master mix and containing the same number and same stage of animals in each tube. To construct *ric-8(md303) dpy-20(e1282); pkIs296*, we started with NL545 *dpy-20(e1362); pkIs296* [HS::gsa-1 (Q208L) dpy-20(+)] (Korswagen *et al.* 1998) and replaced *dpy-20(e1362)* in this strain with *dpy-20(e1282)*, because *e1282* males mate better. We then crossed *dpy-20(e1282); pkIs296* males to *ric-8(md303) dpy-20(e1282)* hermaphrodites and used standard methods to produce the final strain. *ceIs6; ric-8(md303)* and *ceIs11; ric-8(md303)* double mutants were confirmed by sequencing the *ric-8(md303)* locus and by confirming that 100% of animals were positive for the GFP cotransformation marker.

Neuronal vacuole counting: Animals that had never been

starved were picked from growing cultures, mounted on 2% agarose pads in 1 mM sodium azide in M9 buffer and viewed using ×40 dry DIC optics on a Zeiss Axioplan upright microscope. The number of neuronal vacuoles in the head ganglia, ventral cord, and tail ganglia were noted and counted. For each strain, 10 animals from each stage (L1/L2, L2/L3, L4, and young adult) were assayed in this way.

Locomotion assays: Standard locomotion assays were performed as previously described using standardized plates and a standardized definition of a body bend (Miller *et al.* 1999). Exaggerated movements in which the animal doubles back on itself during reversal such that the tail touches the anterior of the body in a figure-eight pattern were scored as three body bends (this applied only to the *egl-30* gain-of-function mutants and to strains treated with phorbol esters in this study). For coiling movements, a body bend was counted every 90° around the circle.

To assay *acy-1(pk1279)*-containing strains, synchronized, larval-arrested, homozygous larvae, along with identically staged wild-type and single-mutant control larvae, were collected and assayed for locomotion rate as described (Reynolds *et al.* 2005). For heat-shock locomotion assays four young adults were picked from growing cultures for each of four locomotion assay plates. These plates were heat-shocked at 13-min intervals, and, at the specified times after heat shock, two of the four animals on each plate were randomly chosen, and body bends were counted for 6 min for each animal. To heat-shock, plates were triple sealed with parafilm strips, immersed in a 33° water bath for the specified time, using stacks of 33° equilibrated glass microscope slides to hold each plate completely immersed. At the end of the heat shock, plates were immersed in slushy ice water for 35 sec, dried, and incubated at room temperature for the specified time before beginning the assay.

Video production: Images of worms on agar plates containing OP-50 bacterial lawns were captured using a Sony CCD-IRIS black-and-white video camera mounted on an Olympus SZX-12 stereomicroscope and recorded on a Panasonic AG-DV1000 digital videocassette recorder. Video clips were transferred via a firewire connection to a Macintosh Powerbook G4 and captured as an NTSC file using Final Cut Pro 3 (Apple). Cleaner 6 (Discrete) was then used to crop and trim each clip and to convert them to compressed QuickTime videos.

Drug sensitivity assays: Aldicarb sensitivity assays using the population growth rate method were performed as previously described (Miller *et al.* 1999). Aldicarb and levamisole acute paralysis assays on solid media were performed as previously described (Lackner *et al.* 1999; Nurrish *et al.* 1999), except the concentration of aldicarb and levamisole in the media was 2000 and 800 μM, respectively. For the paralysis assays, aldicarb was added from a 10-mM stock solution in ddH_2O (allowing ~2–3 hr for dissolving before adding to the 55° cooled molten media), and media was made with 20% less water than normal to compensate for the large drug volume. Levamisole was added to 55° cooled molten media from a 200-mM stock solution in ddH_2O. Aldicarb and levamisole-containing plates were seeded with OP-50 on the day that they were poured and stored at room temperature for 2 days, lid side up, before using. Levamisole acute paralysis assays in liquid were carried out in microtiter plates containing 30 μl of 2% agarose in each well and 50 μl of 100 μM levamisole in M9 on top of that. For each of three trials for each strain, three wells of 10 animals per well were loaded over a 3-min period and then the number of animals paralyzed (not thrashing) were counted at the specified intervals. It should be noted that the levamisole resistance of the strains in this study was significantly more pronounced in this liquid assay, when compared to the assay on solid media (*e.g.*, compare Figures 6B and 7B).

RESULTS

Mutations that activate the $G\alpha_q$ or $G\alpha_s$ pathways rescue the paralysis of *ric-8(md303)* mutants and cause coordinated, hyperactive locomotion as single mutants: To further clarify the network of signaling proteins that regulates neurotransmitter release, we undertook two large genetic screens. In one screen, we looked for mutations that could suppress the nearly paralyzed phenotype caused by the *ric-8(md303)* missense mutation. Our choice of this mutant for a suppressor screen was based on RIC-8's upstream role in synaptic Gα signaling and our guess that suppressors of the *ric-8* mutant could reveal new components of the $G\alpha_o$-$G\alpha_q$ signaling network or components of intersecting pathways. In a second screen, we looked for mutants that exhibit the hyperactive phenotypes caused by excessive EGL-30 ($G\alpha_q$) pathway activity. To increase our chances of identifying rare, dominant mutations or rare reduction-of-function mutations in genes with lethal null phenotypes, we did the combined screens at ~27-fold redundancy with respect to gene knockout coverage rates.

The screens yielded a number of interesting mutants, including a group of 10 mutants that appeared to strongly suppress the paralysis of *ric-8(md303)*. By adapting existing *C. elegans* technology (Wicks *et al.* 2001), we developed a method to rapidly map the new mutations, at high resolution, relative to SNPs. By this method we mapped the 10 mutations to four different intervals, each <250 kb (Figure 2, A–D). Then, using candidate gene sequencing, we identified the four genes that contain these mutations. Perhaps not surprisingly, we found that two of the mutations are dominant alleles of *egl-30* ($G\alpha_q$), but all of the remaining mutations fell within the canonical $G\alpha_s$ pathway (Figure 3): three are dominant alleles of *gsa-1* ($G\alpha_s$), two are dominant alleles of adenylyl cyclase (*acy-1*), and three are recessive alleles of *kin-2* (regulatory subunit of protein kinase A).

Although the extent of suppression varied significantly between the different mutants, the strongest *gsa-1* mutations, remarkably, transformed the nearly paralyzed *ric-8(md303)* mutants into strains that were significantly more active than the wild-type strain, resulting in an ~40-fold improvement in locomotion rate, and when we transferred the suppressor mutations out of the *ric-8* mutant background into a wild-type background, we found that all of the mutations conferred continuous, strongly hyperactive and highly coordinated locomotion as single mutants (Figure 4, A and B, and Figure 4 supplemental QuickTime movies at http://www.genetics.org/supplemental/). *ce94* appears to be the strongest *gsa-1* gain-of-function mutation that we isolated on the basis of the fact that *ce94*/+ heterozygotes are significantly more hyperactive than *ce81*/+ heterozygotes.

The *egl-30*, *gsa-1*, and *acy-1* mutations all exhibited strong dominance (Figure 4C). Indeed, strains heterozy-

gous for the *acy-1(ce2)* and *gsa-1(ce94)* mutations were as hyperactive, or more hyperactive, respectively, than the corresponding homozygous strains. The hyperactive locomotion conferred by the dominant *egl-30*, *gsa-1*, and *acy*-1 mutations described here is the opposite of the sluggish/paralyzed phenotype conferred by reduction or loss-of-function mutations in these genes (Table 2). This suggests that these mutations promote a gain-of-function activation of each protein and therefore that the suppression of *ric-8(md303)* is caused by these mutations promoting activation of the $G\alpha_q$ or $G\alpha_s$ pathways. Further genetic analysis supports this inference. The gain-of-function nature of the *egl-30* ($G\alpha_q$) and *gsa-1* ($G\alpha_s$) mutations is suggested by our finding that they promote hyperactive locomotion when present at a single copy per genome in a manner similar to, or greater than, strains that overexpress wild-type transgenic versions of these genes (Figure 4, A and C; Korswagen *et al.* 1997; Bastiani *et al.* 2003). Supporting the gain-of-function nature of the *acy-1* mutations, we found that introducing the *ce2* mutation into wild-type worms on a transgene caused hyperactive locomotion (shown later in Figure 10A), whereas a wild-type version of *acy-1* did not obviously affect locomotion rate, even at significantly higher transgene doseages (data not shown). Although this result alone does not rule out the possibility that the *acy-1* alleles might have an altered (neomorphic) function, their strong similarity to the other $G\alpha_s$ pathway activating mutations, and the fact that they confer the opposite phenotype from loss-of-function mutants (Table 2), argues that they are also true gain-of-function alleles. In contrast, the recessive *kin-2* mutations are reduction-of-function alleles, because a transgene containing a wild-type copy of the *kin-2* gene rescues the *kin-2* mutant phenotypes, including the ability of the *kin-2* mutations to suppress *ric-8(md303)* (Figure 4A).

$G\alpha_s$ is completely dependent on adenylyl cyclase to regulate growth and locomotion: As shown in Figure 4, the strong *gsa-1* ($G\alpha_s$) gain-of-function mutations suppress the paralysis of *ric-8(md303)* mutants significantly better than the gain-of-function mutations in *acy-1*. This could indicate that $G\alpha_s$ has other effectors in addition to adenylyl cyclase, or it could simply indicate that the mutations activate the pathway to different degrees. To address whether or not other $G\alpha_s$ effectors contribute significantly to the regulation of locomotion, we constructed a double mutant containing a strong *gsa-1* ($G\alpha_s$) activating mutation in combination with an *acy-1* null mutation. A previous study produced the *acy-1(pk1279)* mutation and showed that it deletes the *acy-1* gene and causes larval lethality and paralysis that can be rescued with the wild-type *acy-1* gene (Moorman and Plasterk 2002). Interestingly, the *acy-1(pk1279)* null mutation actually increases life span; the larval arrest results from failure to progress to the adult stage (Moorman and Plasterk 2002). The paralysis conferred by the *acy-1*

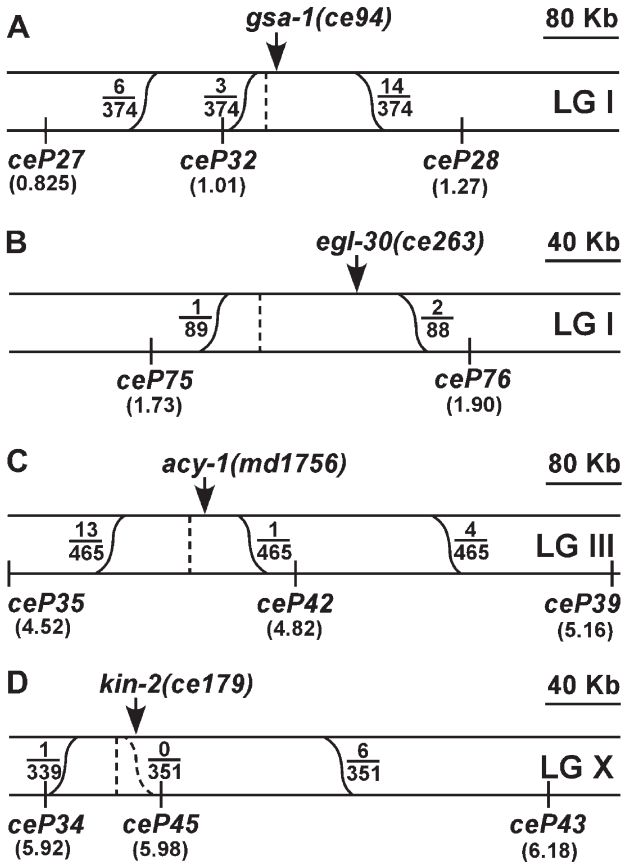

Figure 2.—Summary of SNP fine-mapping data for four new synaptic signaling network mutations. (A–D) Regions of 320 kb (B and D) or 640 kb (A and C) near each mutation. The chromosome on which each mutation resides is indicated on the right as LG I, III, or X. The top strand represents the mutant chromosome, and the bottom strand represents the CB4856 chromosome containing the indicated SNP markers. This is the expected arrangement of the two chromosomes during the crossing-over stage of meiosis when recombination could occur. Sinusoidal lines represent recombination events that could place the mutation on the same chromosome as an SNP marker. Fractions represent the number of actual recombination events, inferred from SNP mapping data, over the total number of homozygous mutant lines tested. The vertical dashed line in A–D represents the predicted location of each mutation, which we extrapolated from the fraction of recombination events that occurred on each side of the mutation. The arrow in A–D points to the actual location of the mutation based on sequencing studies described herein. The numbers in parentheses under each SNP marker indicate the distance of each marker, in units of millions of base pairs, from the left end of the chromosome (taken from WormBase Release WS91). We also mapped the other six *ric-8* suppressor mutations that were analyzed in this study as follows: *ce81* and *ce218* both map to the same region as *ce94*, between *ceP27* and *ceP28* (A); *ce41* maps to the same interval as *ce263*, between *ceP75* and *ceP76* (B); *ce2* maps to the same region as *md1756*, between *ceP35* and *ceP39* (C); and *ce38* and *ce151* fail to complement *ce179* (D) and show tight linkage to *ce179* (no wild-type progeny observed among progeny of *ce179/ce38*). See Table 1 for details of the SNP markers shown in this figure.

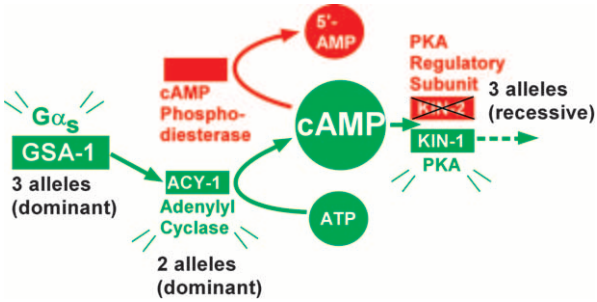

FIGURE 3.—Pathway model of the *C. elegans* $G\alpha_s$ pathway. Shown are the *C. elegans* orthologs of the canonical $G\alpha_s$ pathway that are relevant to this study, arranged as originally defined by vertebrate biochemical studies, which is consistent with this study and previous *C. elegans* genetic studies (BERGER *et al.* 1998; KORSWAGEN *et al.* 1998). According to the model, GSA-1 ($G\alpha_s$)'s action is mediated, in whole or part, by its major effector molecule ACY-1. ACY-1 produces the small signaling molecule cAMP. The binding of cAMP to KIN-2 (a PKA regulatory subunit) leads to its dissociation from the inactive holoenzyme and the release of active KIN-1 (a PKA catalytic subunit). Other potential effectors of cAMP are not shown. cAMP action is terminated by one or more cAMP phosphodiesterases (not identified). Activating green proteins or reducing the function of red proteins suppresses *ric-8(md303)*. For each component, the number of alleles that this study identified is indicated, along with allele type (dominant or recessive).

(pk1279) mutation results from functional, rather than permanent developmental, defects (REYNOLDS *et al.* 2005).

When we moved the *acy-1(pk1279)* mutation into the *gsa-1(ce81)* background, we found that the double mutant was essentially indistinguishable from the *acy-1 (pk1279)* single mutant with respect to overall appearance, and, as Figure 5 shows, the locomotion rate of *acy-1 (pk1279)* was not improved by the *gsa-1(ce81)* mutation. This suggests that there are no other major effectors in addition to ACY-1 through which GSA-1 can signal to regulate locomotion rate. Similarly, we found that the *gsa-1* strong gain-of-function mutation could not bypass the larval arrest phenotype of *acy-1* nulls, although the *gsa-1(ce81); acy-1(pk1279)* double mutants, like *acy-1 (pk1279)* single mutants, can survive for days after hatching (REYNOLDS *et al.* 2005). Although our genetic analysis does not address whether or not GSA-1 directly activates ACY-1, as biochemical studies have shown with vertebrate homologs (*e.g.*, TESMER *et al.* 1997), these results are consistent with ACY-1 being the major effector by which GSA-1 ($G\alpha_s$) regulates growth and locomotion rate.

Molecular analysis of *ric-8(md303)* suppressor mutations reveals both known and novel gain-of-function mutations in the $G\alpha_q$ and $G\alpha_s$ pathways: To investigate the mechanisms by which the *ric-8* suppressor mutations activate the $G\alpha_q$ and $G\alpha_s$ pathways, we undertook a molecular analysis of each mutation in the context of available structural data. Our three dominant mutations in GSA-1 ($G\alpha_s$) are all missense alleles that are predicted to interfere with GTP hydrolysis and thus should cause the protein to become stuck in the GTP-bound "ON" position (Figure 6A; Table 3). *gsa-1(ce94)* (G45R) changes a Gly in the phosphate-binding P-loop that binds the $\beta\gamma$ phosphates of GTP (VETTER and WITTINGHOFER 2001). Interestingly, this Gly is completely conserved in all G proteins, including small G proteins such as ras, where it corresponds to Gly12, a common site for ras gain-of-function mutations in human tumors (BOS 1989). The other two mutations affect two of the three residues that are proposed to form the catalytic triad for GTP hydrolysis (SONDEK *et al.* 1994). *gsa-1(ce81)* (R182C) mutates the catalytic Arg. This Arg is the target of ADP ribosylation by cholera toxin (VAN DOP *et al.* 1984). Indeed, R182C is known to inhibit GTP hydrolysis, both *in vitro* and in human disease, where it is found in individuals with McCune-Albright syndrome, and in certain kinds of growth-hormone-secreting human pituitary tumors (LANDIS *et al.* 1989; LYONS *et al.* 1990; SHENKER *et al.* 1993). The *gsa-1(ce218)* mutation (T185A) also affects the catalytic triad; however, this mutation suppresses *ric-8(md303)* more weakly than do the *ce81* and *ce94* mutations (Figure 4A).

One of our dominant mutations in EGL-30 ($G\alpha_q$) also changes residues in a region known to be important for GTP hydrolysis (Figure 6A; Table 3). The *egl-30(ce263)* (E208K) mutation is located just three amino acids downstream of the catalytic glutamine. This residue is conserved among all Gα proteins, but not in ras.

Our two dominant mutations in ACY-1 both change conserved residues in the C1 catalytic domain (Figure 6B; Table 3). Adenylyl cyclase is composed of two soluble catalytic domains (C1 and C2) connected to 12 transmembrane helices (TAUSSIG and GILMAN 1995). Previous studies have shown that the activation of adenylyl cyclase requires the coming together of the C1 and C2 domains, and previous dominant mutations have been found to increase the affinity of the two domains for each other (HATLEY *et al.* 2000). We note that the *acy-1 (md1756)* mutation occurs at a known contact point between the two domains, as revealed by structural studies of vertebrate adenylyl cyclases (TESMER *et al.* 1997; ZHANG *et al.* 1997). Our two strongest recessive mutations in KIN-2 (a regulatory subunit of protein kinase A) both change conserved residues in the four-amino-acid inhibitory pseudosubstrate domain that normally functions to keep protein kinase A turned off in the absence of cAMP (Figure 6C; Table 3). Biochemical studies in vertebrates have shown that the Arg mutated in *kin-2(ce179)* (R92C) and conserved from yeast to humans is critical for the regulatory subunit to exert its inhibitory effects and that mutating it results in a holoenzyme that is extremely hypersensitive to cAMP (BUECHLER *et al.* 1993); however, none of our *kin-2* mutations are likely to be null mutations, because we

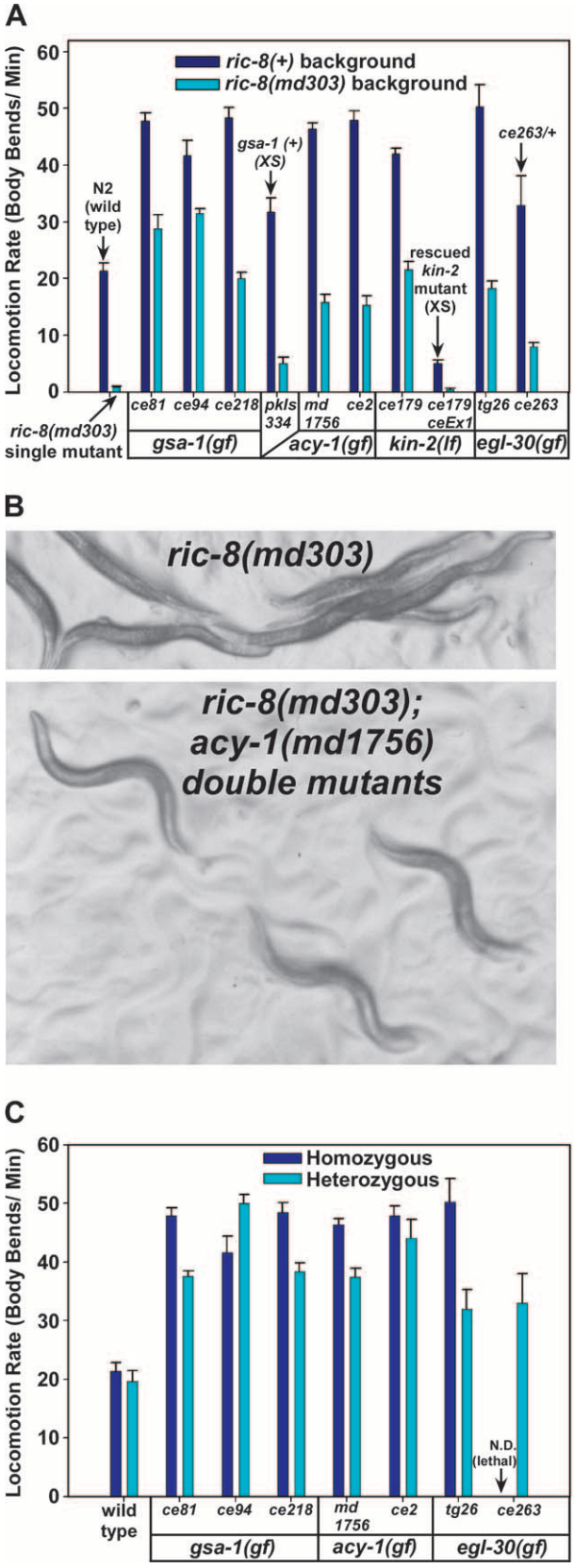

FIGURE 4.—Mutations that activate the $G\alpha_s$ or $G\alpha_q$ pathways strongly suppress the paralysis of *ric-8(md303)* mutants and cause hyperactive locomotion in a *ric-8(+)* background. (A) Shown are the mean locomotion rates, expressed as body bends per minute, of strains carrying various mutations that activate the $G\alpha_s$ or $G\alpha_q$ pathways. *egl-30(tg26)* was isolated in a previous study (DOI and IWASAKI 2002). Dark-blue bars represent the mutants in a *ric-8(+)* (wild type for *ric-8*) background, while cyan bars represent double mutants carrying the indicated mutations in a *ric-8(md303)* (strong reduction-of-function) background. For comparison, wild-type animals (N2) and *ric-8(md303)* single mutants are shown in the first set of two bars, as indicated. Allele names are indicated and are grouped according to the affected genes. Allele types [gain of function (gf) or loss of function (lf)] are indicated for each gene. The two strongest *gsa-1* gf mutations improve the locomotion rate of *ric-8(md303)* mutants ~40-fold and confer significantly hyperactive locomotion even in a *ric-8(md303)* background (in comparisons of N2 wild type *vs. gsa-1(ce94); ric-8(md303)* or *gsa-1(ce81); ric-8(md303)* double mutants, the *P*-values are <0.0001 and 0.0222, respectively, using the unpaired *t*-test with Welch correction). Strains carrying transgenic arrays that overexpress *gsa-1(+)* or *kin-2(+)* are indicated with arrows and the annotation "XS." Note that overexpression of the *kin-2(+)* gene in either the *ric-8(+)* or the *ric-8(md303)* background rescues the *kin-2* loss-of-function locomotion phenotype and confers sluggish locomotion. As indicated, the *egl-30* gain-of-function mutation *ce263* has been assayed only as a heterozygote in the *ric-8(+)* background, because heterozygotes are larval lethals. Not included are data for two weaker alleles of *kin-2* (*ce38* and *ce151*) and one weaker gain-of-function allele of *egl-30(ce41)*. Error bars represent the standard error of the mean for 8–10 animals. See also supplemental QuickTime movies for Figure 4 at http://www.genetics.org/supplemental/. (B) Images comparing the posture and movement of *ric-8(md303)* single mutants and *ric-8(md303); acy-1(md1756)* double mutants. While *ric-8(md303)* mutants exhibit a relatively flat waveform and a straight, paralyzed posture, the double mutants exhibit postures not readily distinguishable from wild type (not shown). (C) Mutants carrying gain-of-function mutations in the $G\alpha_s$ or $G\alpha_q$ pathways exhibit strong dominance. Shown are the mean locomotion rates, expressed as body bends per minute, of strains carrying various mutations that activate the $G\alpha_s$ or $G\alpha_q$ pathways. Dark blue and cyan bars represent animals homozygous or heterozygous, respectively, for the indicated mutations. All heterozygotes are also heterozygous for *dpy-5(e61)*, which was used as a recessive marker mutation to identify heterozygotes. For comparison, wild type (N2) and *dpy-5(e61)/+* are shown in the first set of two bars. Allele names are indicated and are grouped according to the affected genes. Note that all of these mutations confer significantly hyperactive locomotion even in heterozygous strains (highest *P*-value for any strain when compared to wild type is 0.051 for the *egl-30(ce263)/+* mutant). Note that mutants carrying the *gsa-1(ce94)* mutation are significantly more hyperactive as heterozygotes than as homozygotes ($P = 0.021$). The notation "*ce263/+*" indicates that the *egl-30(ce263)* gain-of-function mutation has not been assayed in a homozygous state outside of the *ric-8(md303)* background in which we isolated it (because strains heterozygous for this mutation in a *ric-8(+)* background do not reach adulthood). Error bars represent the standard error of the mean for 10 animals. Statistical comparisons use the unpaired *t*-test with Welch correction.

found that *kin-2* RNAi confers a larval arrest loss-of-function phenotype.

In summary, our findings of strong dominance, our comparisons to loss-of-function phenotypes, our molecular analyses, and our transgenic experiments demonstrate that the mutations in EGL-30, GSA-1, and ACY-1

TABLE 2

Locomotion rates conferred by selected gain-of-function and null mutations in the *C. elegans* $G\alpha_q$ and $G\alpha_s$ signaling pathways

Protein	Mutant genotype	Reference for mutation isolation	Effect of mutation	Locomotion rate (body bends/min)[a]
–	N2 (wild type)	–	+	21.3 ± 1.5
EGL-30 ($G\alpha_q$)	*egl-30(tg26)*	Doi and Iwasaki (2002)	Gain of function	50.3 ± 4.0
EGL-30 ($G\alpha_q$)	*egl-30(ad810)*	Brundage *et al.* (1996)	Putative null	0.024 ± 0.003[b]
GSA-1 ($G\alpha_s$)	*gsa-1(ce81)*	This study	Gain of function	47.9 ± 1.3
GSA-1 ($G\alpha_s$)	*gsa-1(pk75)*	Korswagen *et al.* (1997)	Null	ND[c]
ACY-1	*acy-1(ce2)*	This study	Gain of function	48.0 ± 1.6
ACY-1	*acy-1(pk1279)*	Moorman and Plasterk (2002)	Null	0.75 ± 0.10[b]

Note the opposite effects on locomotion rate conferred by gain-of-function and null mutations in each of these genes.

[a] Mean ± standard error. $N \geq 10$ animals.

[b] The paralysis of these mutants is not caused by general sickness, muscle, or developmental defects, because they can be acutely rescued to wild-type levels of locomotion by manipulating Gα pathway signaling (Reynolds *et al.* 2005, accompanying article in this issue).

[c] These mutants exhibit early larval paralysis and death caused by an apparent problem in fluid balance (Korswagen *et al.* 1997).

all promote a gain-of-function activation of each protein, while the recessive KIN-2 mutations, rescueable with wild-type transgenes, are reduction of function, although, as demonstrated by the vertebrate biochemical studies, they should indirectly cause hyperactivation of protein kinase A. Therefore, the *ric-8(md303)* suppressor mutations described herein are mutations that enhance or activate signaling in the $G\alpha_q$ or $G\alpha_s$ pathways.

Native $G\alpha_s$ pathway activating mutations cause minimal neuronal cell death: We were not surprised to find that activating the $G\alpha_q$ pathway could suppress *ric-8* mutants, because in a previous study we showed that knocking out negative regulators of the EGL-30 ($G\alpha_q$) pathway or exogenous application of phorbol esters could suppress *ric-8* mutants (Miller *et al.* 2000). However, we were surprised to find that activating the $G\alpha_s$ pathway could suppress *ric-8* mutants, because previous transgenic studies in *C. elegans* demonstrated that $G\alpha_s$ gain-of-function mutations can kill neurons and cause permanent paralysis (Korswagen *et al.* 1997; Berger *et al.* 1998). Do the native *gsa-1* gain-of-function mutations kill neurons? When we used Nomarski microscopy to look for signs of neuronal cell death in these mutants, we found that they did have significantly more neuronal vacuoles (an indicator of dead or dying neurons) than wild type; but, on average, only ~1 of the ~300 nerve cells in each animal was affected (Figure 7). This is much lower than the transgenic $G\alpha_s$ gain-of-function strains, in which about half of the neurons were killed (Korswagen *et al.* 1997; Berger *et al.* 1998). Furthermore, we found that the number of neuronal vacuoles did not significantly increase as the *gsa-1* mutants developed (Figure 7). So, unlike the transgenic strains, the native dominant mutations do not cause widespread neuronal death, as seems self-evident from the hyperactive locomotion phenotype.

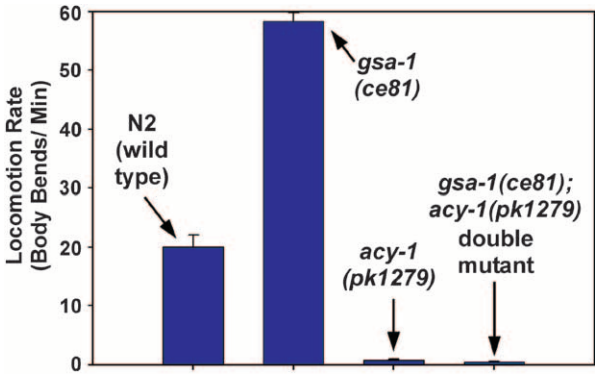

Figure 5.—$G\alpha_s$ is completely dependent on adenylyl cyclase to regulate locomotion rate. Shown are the mean locomotion rates, expressed as body bends per minute, of the wild-type strain and strains carrying the *gsa-1(ce81)* and/or *acy-1(pk1279)* mutations. Error bars represent the standard error from populations of 8–10 larvae (each 6–30 hr old).

Activating the $G\alpha_s$ pathway suppresses *ric-8(md303)* by inducing rapid functional changes: What is the function of the $G\alpha_s$ pathway at the synapse, and why do mutations that activate it cause hyperactive locomotion and strongly suppress *ric-8(md303)*? To begin to address this question, we first asked if the suppression of *ric-8 (md303)* is the result of permanent developmental changes that occur as the *ric-8* mutants develop in the presence of an activated $G\alpha_s$ pathway or, alternatively, if the suppression is caused by "real-time" functional changes that can be induced at any stage by activating the $G\alpha_s$ pathway. To test this, we crossed a transgene containing a *gsa-1* gain-of-function mutation under control of a heat-shock-inducible promoter (Korswagen *et al.* 1997) into the *ric-8(md303)* mutant background. In the absence of heat shock, these animals were only slightly more active than *ric-8(md303)* single mutants, apparently as a result of slight leakiness of the heat-shock promoter (Figure 8). In contrast, only 3 hr after a

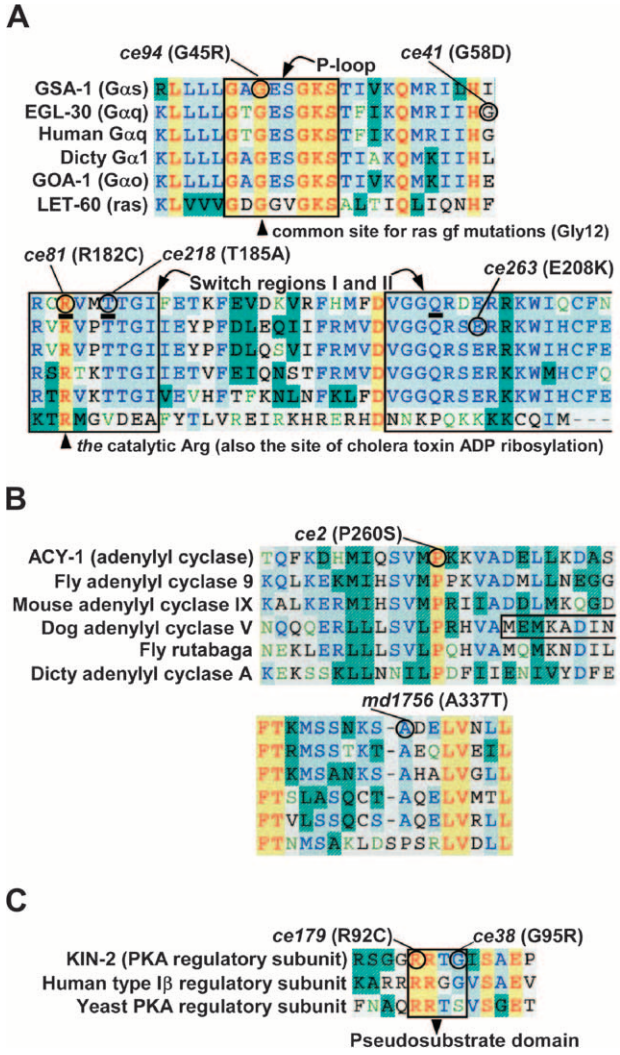

FIGURE 6.—Molecular analysis of *ric-8(md303)* suppressor mutations reveals both known and novel gain-of-function mutations in the $G\alpha_s$ and $G\alpha_q$ pathways. (A) Gain-of-function mutations in GSA-1 ($G\alpha_s$) and EGL-30 ($G\alpha_q$) disrupt residues critical for GTP hydrolysis. Shown are amino acid sequence alignments of two regions relevant to the Gα mutations described herein. Residues that are identical in all six proteins are highlighted yellow, those identical in five of six are highlighted light blue, and other colors indicate various degrees of less-conserved residues. The boxed area labeled "P-loop" in the upper alignment indicates the boundaries of the phosphate-binding loop that binds the βγ phosphates of GTP (VETTER and WITTINGHOFER), which is thought to participate in stabilizing a pentavalent intermediate of GTP hydrolysis (SONDEK *et al.* 1994). Boxes in the lower alignment delineate the boundaries of two of the three moveable switch elements that are directly involved in GTP hydrolysis, as defined by SUNAHARA *et al.* (1997). The three residues underlined in the GSA-1 ($G\alpha_s$) sequence correspond to residues proposed to form the pentavalent intermediate active site for GTP hydrolysis (SONDEK *et al.* 1994). GSA-1 ($G\alpha_s$) and EGL-30 ($G\alpha_q$) gain-of-function mutations identified in this study are circled, and the specific amino acid change is stated. Note that two of the three *gsa-1* gain-of-function mutations identified in this study change active site residues. Arrowheads point to amino acids corresponding to a common site of ras gain-of-function mutations (which is the same residue mutated in *gsa-1(ce94)*) and the catalytic arginine that is ADP ribosylated by cholera toxin, which is mutated in *gsa-1(ce81)*). Accession numbers for the six proteins (from top to bottom) are GI:2443297, U56864, P50148, M25060, M38251, and A36290. (B) Gain-of-function mutations in ACY-1 change conserved residues in the C1 catalytic domain. Shown are amino acid sequence alignments of two regions in adenylyl cyclase's C1 catalytic domain that are relevant to the mutations described herein. The aligned sequences in each region, as indicated, include *C. elegans* ACY-1, mouse and fly orthologs of ACY-1 (known as type IX adenylyl cyclase), dog adenylyl cyclase V, the fly rutabaga gene product, and Dictystelium adenylyl cyclase A. A three-sided box in the dog adenylyl cyclase V sequence indicates the start of the C1 region that was used for a previous structural study (TESMER *et al.* 1997). Note that the *ce2* gain-of-function mutation changes an absolutely conserved Pro residue near the beginning of the C1 domain. The *md1756* mutation changes a conserved Ala residue that corresponds to a known contact point between the C1 and C2 domains, as revealed by structural studies (TESMER *et al.* 1997; ZHANG *et al.* 1997). Accession numbers for the six proteins (from top to bottom) are CAA84795, AF005630, AAC52603, M88649, M81887, and Q03100. (C) Strong reduction-of-function mutations in KIN-2 (regulatory subunit of protein kinase A) change conserved residues in the small, inhibitory pseudosubstrate domain. Shown is an amino acid sequence alignment centered around the pseudosubstrate domain. The aligned sequences include *C. elegans* KIN-2, its human ortholog (type Iβ PKA regulatory subunit), and the yeast PKA regulatory subunit. Both the *ce179* and the *ce38* mutations fall within the four-amino-acid boxed region known as the pseudosubstrate domain. The *kin-2(ce151)* mutation (E137K; not shown) falls outside of the region shown. Note that the *ce179* mutation changes an absolutely conserved Arg. Accession numbers for the three proteins (from top to bottom) are P30625, P31321, and NC_001141.

40-min heat-shock treatment, *ric-8(md303)* adult animals containing the *gsa-1* gain-of-function transgene were, astonishingly, moving at locomotion rates slightly greater than that of the wild-type strain (Figure 8 and Figure 8 supplemental movies at http://www.genetics.org/supplemental/). The locomotion rates of wild-type and *ric-8(md303)* single-mutant controls were unchanged 3 hr after the heat shock. We observed similar results upon heat-shock induction of the *gsa-1* gain-of-function transgene in larval *ric-8(md303)* animals (data not shown). In a wild-type background, heat-shock induction of the *gsa-1* gain-of-function transgene in adults caused hyperactive locomotion (Figure 8). We conclude that both the hyperactive locomotion and the strong suppression of *ric-8(md303)* that occurs upon activating the $G\alpha_s$ pathway is largely, if not entirely, the result of relatively rapid changes.

The hyperactivated $G\alpha_s$ pathway does not strongly suppress the paralysis of presynaptic mutants with defects in synaptic vesicle docking or priming: To further investigate why activating the $G\alpha_s$ pathway strongly rescues the paralysis of *ric-8(md303)* mutants, we tested the specificity of the suppression by asking if the $G\alpha_s$ pathway activating mutations could rescue the near paralysis of mutants with defects in synaptic vesicle docking or priming. The locomotion rate of *ric-8(md303)* is improved

TABLE 3

Summary of *ric-8(md303)* suppressor mutations that activate the $G\alpha_s$ or $G\alpha_q$ pathways

Allele name	Allele type	Affected protein	Amino acid change	Region disrupted
egl-30(ce41)	Gain of function	EGL-30 ($G\alpha_q$)	G58D	11th amino acid downstream from P-loop
egl-30(ce263)	Gain of function	EGL-30 ($G\alpha_q$)	E208K	Switch region II; third amino acid downstream from the catalytic glutamine
gsa-1(ce94)	Gain of function	GSA-1 ($G\alpha_s$)	G45R	P-loop mutation. Glycine is conserved in ras, where it is known as Gly12, and is a common site for ras gain-of-function mutations in human cancers
gsa-1(ce81)	Gain of function	GSA-1 ($G\alpha_s$)	R182C	Switch region I; this is the catalytic Arg and also the site of cholera toxin ADP ribosylation, and this same mutation is found in human pituitary tumors
gsa-1(ce218)	Gain of function	GSA-1 ($G\alpha_s$)	T185A	Switch region I; this is the catalytic Thr.
acy-1(ce2)	Gain of function	ACY-1	P260S	Near the beginning of the C1 catalytic domain
acy-1(md1756)	Gain of function	ACY-1	A337T	C1 catalytic domain. A known point of contact between the C1 and C2 catalytic domains
kin-2(ce179)	Reduction of function	KIN-2 (PKA regulatory subunit)	R92C	Pseudosubstrate domain; this Arg is known to be critical for inhibition of protein kinase A
kin-2(ce38)	Reduction of function	KIN-2 (PKA regulatory subunit)	G95R	Pseudosubstrate domain that normally functions to keep protein kinase A turned off in absence of cAMP
kin-2(ce151)	Reduction of function	KIN-2 (PKA regulatory subunit)	E137K	Region between pseudosubstrate domain and cAMP binding sites

Strongest pathway activators are underlined. See also Figure 6.

up to 40-fold by activating the $G\alpha_s$ pathway, but the locomotion rate of the synaptic vesicle priming mutant *unc-13(s69)*, a strong reduction-of-function mutant (Richmond *et al.* 1999; Kohn *et al.* 2000), is improved only ~4-fold by activating the $G\alpha_s$ pathway (Figure 9A). This slight suppression amounted to a nearly complete block of the $G\alpha_s$ pathway with respect to locomotion rate, because the locomotion rate of the *gsa-1(ce81); unc-13(s69)* double mutant was only ~2% of the *gsa-1(ce81)* single mutant. In addition, activating the $G\alpha_s$ pathway restored, to all appearances, perfectly coordinated locomotion in *ric-8(md303)* mutants, whereas the movement of *gsa-1(ce81); unc-13(s69)* double mutants was uncoordinated (Figure 9 supplemental movies at http://www.genetics.org/supplemental/). Similar results were obtained with *unc-18* null mutants (Figure 9 and Figure 9 supplemental movies at http://www.genetics.org/supplemental/), in which synaptic vesicle docking is disrupted (Weimer *et al.* 2003). In addition to highlighting the specificity of the suppression of *ric-8(md303)*, these results demonstrate that the $G\alpha_s$ pathway is largely dependent on the synaptic vesicle priming mechanism to exert its effects on locomotion.

Hyperactivating the $G\alpha_s$ pathway increases steady-state neurotransmitter release: Is the hyperactive locomotion and strong suppression of *ric-8(md303)* that occurs upon activating the $G\alpha_s$ pathway associated with increased neurotransmitter release, or could altered neurotransmitter receptor responses also contribute? The major excitatory neurotransmitter at *C. elegans* neuromuscular junctions is acetylcholine (ACh). Therefore, to address this question, we first tested the responses of the $G\alpha_s$ pathway activation mutants to the acetylcholine receptor agonist levamisole, and we found that they are all significantly resistant to the paralytic effects of levamisole (Figure 9B). Similar results were obtained with the ACh receptor agonist nicotine (data not shown). Although this seems to support the idea that the hyperactive locomotion of these mutants is not the result of increased sensitivity of the muscle to ACh, it could also mean that these mutants are simply able to tolerate higher amounts of receptor stimulation without becoming paralyzed.

To test for increased steady-state neurotransmitter release in the $G\alpha_s$ pathway activation mutants, we assessed their sensitivities to the acetylcholinesterase inhibitor aldicarb. Since the secreted ACh that accumulates in the presence of aldicarb is toxic, mutations that decrease or increase the rate of ACh secretion confer resistance or hypersensitivity to aldicarb, respectively (Rand and Nonet 1997). When we measured the aldicarb sensitivities of the mutants with an activated $G\alpha_s$

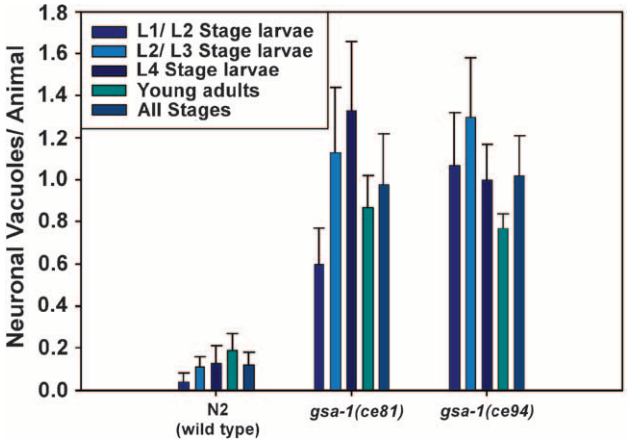

FIGURE 7.—Native gain-of-function mutations do not cause widespread neuronal death. Shown is the average number of neuronal vacuoles per animal in wild type and in our two strongest *gsa-1* gain-of-function mutants. The results show that these mutants have significantly more neuronal vacuoles than wild type (the *P*-values are 0.0002 and <0.0001 for comparing N2 to *gsa-1(ce81)* and *gsa-1(ce94)*, respectively, using the unpaired *t*-test with Welch correction); however, the level of neuronal death amounts to, on average, only ~1 of ~300 nerve cells in each animal. Also note that the number of neuronal vacuoles did not significantly increase as the mutants developed into young adults. Error bars represent the standard error of the means for a sample size of 10 animals.

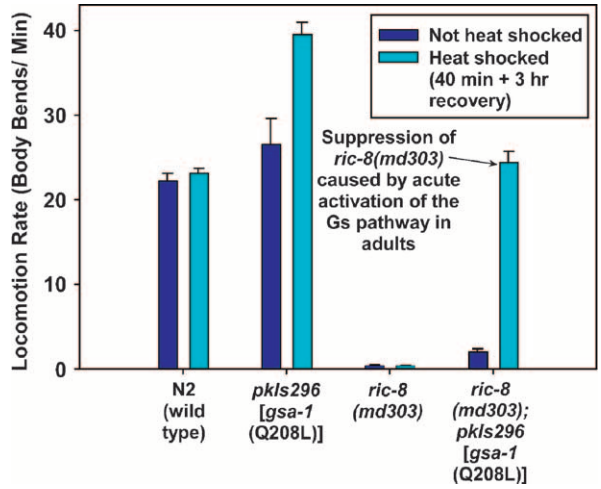

FIGURE 8.—Activating the $G\alpha_s$ pathway suppresses *ric-8(md303)* and causes hyperactive locomotion by inducing rapid functional changes. A transgenic array carrying the *gsa-1* Q208L gain-of-function mutation under control of a heat-shock-inducible promoter [HS::gsa-1(Q208L)] suppresses *ric-8(md303)* only 3 hr after a 40-min heat-shock treatment. Dark blue and cyan bars indicate locomotion rates without or with heat-shock treatment, respectively. Note that the heat-shock induction of *gsa-1* (Q208L) improves the locomotion rate of *ric-8(md303)* ~13-fold relative to non-heat-shock conditions, whereas heat-shock treatment of control strains does not improve locomotion rate. Heat-shock induction of *gsa-1* (Q208L) in a *ric-8(+)* background causes significantly hyperactive locomotion. The slightly improved locomotion rate associated with the array under non-heat-shock conditions (relative to control strains) may indicate that the promoter is not completely off under non-heat-shock conditions. Error bars represent the standard error of the mean for eight animals. See also supplemental QuickTime movies for Figure 8 at http://www.genetics.org/supplemental/.

pathway, we found that they all are hypersensitive to aldicarb at all concentrations tested (Figure 9C). This result suggests that these strains release abnormally high levels of the neurotransmitter acetylcholine. Is increased neurotransmitter release related to the suppression of *ric-8(md303)*? This seems to be the case, because *ric-8(md303)* releases abnormally low levels of acetylcholine, as indicated by its strong resistance to aldicarb, and yet activating the $G\alpha_s$ pathway in *ric-8(md303)* seems to restore steady-state neurotransmitter release to levels in excess of wild type (Figure 9C).

Suppression of *ric-8(md303)* occurs via the neuronal $G\alpha_s$ pathway, but both the muscle and nervous system $G\alpha_s$ pathways contribute to the locomotion rate and drug sensitivity phenotypes: The *C. elegans* GSA-1 ($G\alpha_s$) pathway is expressed in both nervous system and body-wall muscle cells. To investigate the relative contributions of these two tissues to the suppression, locomotion, and drug sensitivity phenotypes associated with an activated $G\alpha_s$ pathway, we reproduced the *ce2* (P260S) mutation on a full-length *acy-1* cDNA and then made transgenic animals carrying this gain-of-function mutation under control of muscle and/or nervous system specific promoters. Expressing the *acy-1* (P260S) cDNA under control of the *rab-3* nervous system specific promoter caused hyperactive locomotion in a wild-type background as well as strong suppression of the paralysis of *ric-8(md303)* (Figure 10A). Surprisingly, however, expressing the *acy-1* (P260S) cDNA under control of the *myo-3* muscle-specific promoter also conferred hyperactive locomotion in a wild-type background (Figure 10A). This is not caused by "leaking" of the muscle promoter in nervous system tissue, because control experiments, done as part of a separate study, showed that the *myo-3* promoter, even at high levels, cannot drive rescue of a nervous-system-specific mutant (REYNOLDS *et al.* 2005). However, unlike the nervous-system-specific *acy-1* (P260S) transgene, the muscle-specific *acy-1* (P260S) transgene was unable to cause any rescue of the paralysis of *ric-8(md303)* (Figure 10A). These results show that the suppression of *ric-8(md303)* is dependent on activation of the neuronal $G\alpha_s$ pathway.

The hyperactive locomotion conferred by muscle-specific expression of the *acy-1* (P260S) transgene seems to be caused, at least in part, by increased muscle excitability, because the strain containing the muscle-specific *acy-1* (P260S) transgene was significantly hypersensitive to the paralytic effects of levamisole (Figure 10B). In contrast, the strain containing the neuron-specific *acy-1* (P260S) transgene showed normal sensitivity, or slight resistance, to levamisole, and a strain expressing the *acy-1* (P260S) gene under control of its native promoter

(muscle + nervous system) conferred significant resistance to levamisole (Figure 10B). Since expression in either muscle or nervous system alone is not sufficient to reconstitute the levamisole resistance seen with the native mutations that activate the $G\alpha_s$ pathway, these results suggest that it is the combined actions of hyperactivating the muscle and nervous system $G\alpha_s$ pathways, possibly in communication or coordination with each other, that leads to levamisole resistance.

Similarly, expressing the *acy-1* (P260S) mutation only in muscle or only in the nervous system does not appear to significantly alter overall steady-state levels of neurotransmitter release, as measured by aldicarb sensitivity (Figure 10C). Both the genomic *acy-1(ce2)* mutation and a transgene that expresses the same mutation (P260S) under control of the native *acy-1* promoter cause significant hypersensitivity to aldicarb, this time measured using a paralysis assay, but in agreement with previous results using the population growth assay (Figures 9C and 10C). However, when the same mutation is expressed only in muscle cells or only in the nervous system, aldicarb sensitivity is not significantly altered (Fig-

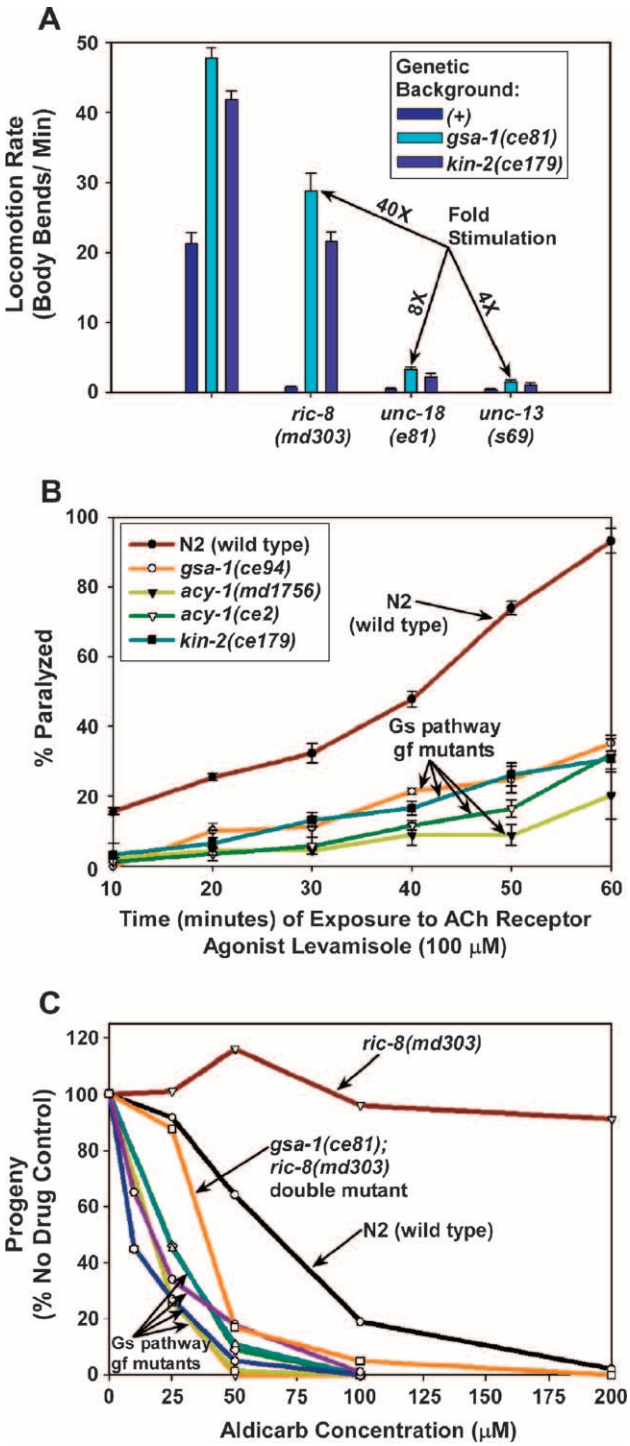

FIGURE 9.—The hyperactivated $G\alpha_s$ pathway increases neurotransmitter release and requires the synaptic vesicle priming protein UNC-13 to exert its effects on locomotion. (A) Activating the $G\alpha_s$ pathway does not strongly suppress the near-paralysis of mutants with reduced synaptic vesicle docking and priming. Shown are the mean locomotion rates, expressed as body bends per minute, of various strains. Strains homozygous for *ric-8(md303)*, *unc-18(e81)*, or *unc-13(s69)* are grouped together as indicated. Dark-blue bars within each set represent strains carrying no additional mutations (genetic background *(+)*). Cyan bars represent double mutants in which the second mutation is *gsa-1(ce81)*, and royal blue bars represent double mutants in which the second mutation is *kin-2(ce179)*. The first group of bars (unlabeled) represents wild-type and single-mutant control strains. "Fold stimulation" calculations are shown only for double mutants carrying the *gsa-1(ce81)* mutation. Error bars represent the standard error of the mean for 8–10 animals. See also supplemental QuickTime movies for Figure 9 at http://www.genetics.org/supplemental/. (B) Mutants with an activated $G\alpha_s$ pathway show reduced sensitivity to the ACh receptor agonist levamisole. The graph compares the percentage of animals that are paralyzed, over a time course, in a solution of 100 μM levamisole. Note that all of the mutants with an activated $G\alpha_s$ pathway are significantly resistant to the paralytic effects of levamisole (all *P*-values are <0.014 for any strain compared to wild type at any time point). This indicates that their hyperactive behavior is not the result of increased sensitivity of the muscle to ACh. Similar results were obtained using 1200 μM nicotine (solution assay) and 800 μM levamisole (solid media assay; data not shown). Error bars represent standard error of the means for three experiments. (C) Hyperactivation of the $G\alpha_s$ pathway causes hypersensitivity to aldicarb. The graph compares the population growth rates of strains with various concentrations of aldicarb. One hundred percent represents the number of progeny produced from a starting population of L1 larvae over a 96-hr period in the absence of aldicarb (carrier only). Note that *ric-8(md303)* is strongly resistant to aldicarb (indicating decreased neurotransmitter release); however, activating the $G\alpha_s$ pathway in the *ric-8* mutant background seems to restore neurotransmitter release to at least wild-type levels, if not greater, since the *gsa-1(ce81); ric-8(md303)* double mutant is hypersensitive to aldicarb. Note that all of the mutants with an activated $G\alpha_s$ pathway (designated "Gs pathway gf mutants") are hypersensitive to aldicarb as single mutants. Mutants included in the cluster designated "Gs pathway gf mutants" are as follows (from left to right at the 40% level): *kin-2(ce179)*, *gsa-1(ce94)*, *gsa-1(ce81)* (superimposed on *ce94*), *kin-2(ce38)*, *acy-1(ce2)*, and *acy-1(md1756)* (superimposed on *ce2*). Curves are representative of duplicate experiments.

ure 10C), despite the fact that these same transgenes cause hyperactive locomotion (Figure 10A). These results suggest that it is the combined actions of hyperactivating the muscle and nervous system $G\alpha_s$ pathways, possibly in communication or coordination with each other, that leads to aldicarb hypersensitivity and increased steady-state neurotransmitter release.

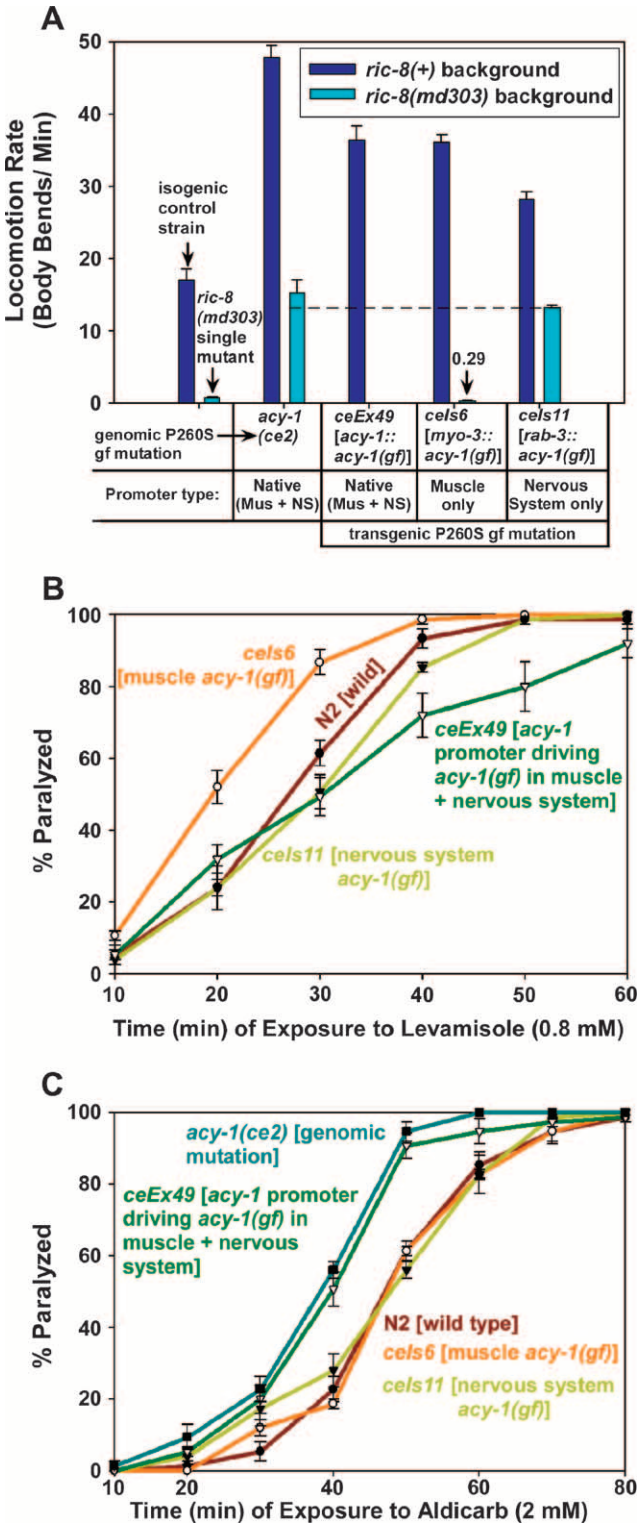

DISCUSSION

In this study, we undertook two large genetic screens aimed at identifying components of the signaling network that regulates neurotransmitter release, and we focused our initial efforts on 10 mutations that strongly suppress the paralysis of *ric-8(md303)* mutants. Through high-resolution SNP-based mapping and candidate gene sequencing, we showed that the mutations affect four proteins—EGL-30 ($G\alpha_q$), GSA-1 ($G\alpha_s$), ACY-1, and KIN-2 (PKA regulatory subunit)—and that the effect of

FIGURE 10.—Suppression of *ric-8(md303)* occurs via the neuronal $G\alpha_s$ pathway, but both the muscle and the nervous system $G\alpha_s$ pathway contribute to the locomotion rate and drug sensitivity phenotypes. (A) Hyperactivation of the $G\alpha_s$ pathway in either muscle or nervous system is sufficient to confer hyperactive locomotion; hyperactivation of the $G\alpha_s$ pathway in the nervous system, but not muscle, significantly suppresses the paralysis of *ric-8(md303)*. Shown are the mean locomotion rates of various strains, expressed as body bends per minute. Dark-blue bars represent a *ric-8(+)* (wild type for *ric-8*) background, while light-blue bars represent a *ric-8(md303)* strong reduction-of-function background. For comparison, the isogenic control strain and the *ric-8(md303)* single mutant are shown in the first set of two bars, as indicated. All remaining bars represent strains carrying the *acy-1* (P260S) gain-of-function mutation either in the form of the *ce2* genomic mutation or on trangenes driven by various promoters, as indicated. All transgenic strains in this figure, including the isogenic control strain, are in the *pha-1(e2123)* background rescued with the *pha-1(+)* gene, which was used as a selectable marker for transformants. Error bars represent the standard error of the mean for 8–10 animals. (B) Both the muscle and the nervous system $G\alpha_s$ pathways contribute to the levamisole resistance phenotype. The graph compares the percentage of animals that are paralyzed, over a time course, on plates containing 800 μM levamisole. Note that a transgene that expresses the same mutation (P260S) under control of the native *acy-1* promoter appears to cause slight resistance to the paralytic effects of levamisole ($P = 0.12$ and 0.09 for the 40- and 50-min time points, respectively). However, the same mutation expressed only in body-wall muscle confers significant hypersensitivity to levamisole ($P = 0.032$ and 0.0071 for the 20- and 30-min time points, respectively), and when expressed only in the nervous system, it either does not significantly alter levamisole sensitivity or causes slight resistance ($P = 0.17$ and 0.11 for the 30- and 40-min time points, respectively). Error bars represent standard error of the means for three experiments. (C) Expressing the *acy-1* (P260S) gain-of-function mutation only in muscle or only in nervous system does not significantly alter overall levels of neurotransmitter release. The graph compares the percentage of animals that are paralyzed, over a time course, on plates containing 2 mM aldicarb. Note that both the genomic *acy-1(ce2)* mutation and a transgene that expresses the same mutation (P260S) under control of the native *acy-1* promoter cause significant hypersensitivity to aldicarb ($P = 0.0055$ and 0.022 for each strain, respectively, at the 50-min time point). However, when the same mutation is expressed only in body-wall muscle or only in the nervous system, aldicarb sensitivity is not significantly altered. Similar results were obtained using the population growth method of measuring aldicarb sensitivity (data not shown). Error bars represent standard error of the means for three experiments.

these mutations is to activate the $G\alpha_q$ or $G\alpha_s$ pathways. Our screens produced the first native, germline $G\alpha_s$ and adenylyl cyclase gain-of-function mutations isolated in an animal system and the first whole-animal nontargeted PKA regulatory subunit mutations.

The results presented in this study do not reveal why activating the $G\alpha_s$ pathway strongly suppresses *ric-8(md303)*. Hindering our understanding of the suppression is the fact that RIC-8 interacts with multiple Gα subunits, including all three major classes of Gα's that are involved in synaptic signaling (Miller *et al.* 2000; Miller and Rand 2000; Klattenhoff *et al.* 2003; Tall *et al.* 2003). In addition, epistasis studies using a *ric-8* null mutant strongly suggest that RIC-8 has an essential role in activating both the $G\alpha_q$ and the $G\alpha_s$ pathways (Reynolds *et al.* 2005). Although we do not know to what extent the $G\alpha_s$ pathway is affected in the non-null *ric-8(md303)* missense mutant, the available evidence indicates that the function of the $G\alpha_q$ pathway is strongly reduced in *ric-8(md303)* mutants, because applying phorbol esters or knocking out negative regulators of the $G\alpha_q$ pathway strongly suppresses the paralysis of *ric-8 (md303)* mutants and restores coordinated locomotion and because steady-state levels of neurotransmitter release are reduced in *ric-8(md303)* mutants to a similar degree as in similarly paralyzed *egl-30* reduction-of-function mutants (Miller *et al.* 2000). In contrast, similarly paralyzed mutants lacking a neuronal $G\alpha_s$ pathway exhibit approximately wild-type levels of steady-state neurotransmitter release and are only partially suppressed for short periods of time by applying phorbol esters or knocking out negative regulators of the $G\alpha_q$ pathway (Reynolds *et al.* 2005). Therefore, although *ric-8(md303)*'s suppression by $G\alpha_s$ pathway activation may partially result from correcting a deficit in $G\alpha_s$ signaling, we think that the activated $G\alpha_s$ pathway must also be compensating, directly or indirectly, for a deficit in $G\alpha_q$ signaling in *ric-8(md303)* mutants. The data discussed in this paragraph therefore suggest a link between the $G\alpha_s$ pathway and the previously discovered $G\alpha_o$-$G\alpha_q$ signaling network.

Activating the $G\alpha_s$ pathway rapidly induces continuous, coordinated, hyperactive locomotion and rapidly rescues the paralysis of *ric-8(md303)* mutants: Our results show that constitutive activation of the $G\alpha_s$ pathway can produce continuous, coordinated and strongly hyperactive locomotion and are in agreement with a previous study, which showed that transgenic overexpression of wild-type *gsa-1* confers hyperactive locomotion (Korswagen *et al.* 1997). However, previous *C. elegans* studies reported widespread neuronal death and paralysis upon transgenic expression of $G\alpha_s$ gain-of-function mutations (Korswagen *et al.* 1997; Berger *et al.* 1998). We think that this was most likely caused by the difficulty in controlling transgene copy number and/or expression levels, since our native mutations conferred only minimal neuronal death and since we were able to produce hyperactive locomotion by controlled heat-shock induction of the same *gsa-1* gain-of-function mutation that was used in the neuronal death studies. Likewise, the sluggish locomotion conferred by a $G\alpha_s$ gain-of-function transgene under control of ectopic promoters in Drosophila larvae could have resulted from expression levels or expression timing factors that were not easily controlled and not optimized for coordinated hyperactive locomotion (Renden and Broadie 2003). Indeed, when we placed wild-type worms on plates containing various concentrations of membrane-permeable cAMP analogs, we were unable to induce hyperactive locomotion and, in fact, high concentrations resulted in sluggish locomotion or paralysis (K. G. Miller, unpublished results). This suggests that the timing and/or location of cAMP elevations is critical with respect to producing cAMP-induced hyperactive locomotion. This is in striking contrast to phorbol esters, which mimic $G\alpha_q$-pathway-produced DAG and cause strongly hyperactive locomotion within 1–2 hr of omnidirectional contact (Miller *et al.* 2000).

Our experiments with a heat-shock inducible $G\alpha_s$ gain-of-function transgene demonstrate that the coordinated, strongly hyperactive locomotion can be induced at any stage, including adulthood, by relatively rapid functional changes on the order of 30 min–3 hr. This is an important point, since its corollary is that the hyperactive locomotion is not dependent on the nervous system developing in the presence of an activated $G\alpha_s$ pathway. A previous study found increased numbers of terminal varicosities and branches in Drosophila *dunce* (cAMP phosphodiesterase) mutants, which have increased levels of cAMP (Zhong *et al.* 1992). Although our studies do not rule out that the $G\alpha_s$ pathway can change nervous system structure, especially at the synaptic ultrastructural level, as has been previously reported (Renger *et al.* 2000), they do suggest that any important changes that it induces occur relatively rapidly and need not be coordinated with neuronal development. Similarly, we also showed that the strong suppression of *ric-8(md303)* occurs independently of development. This is important because it shows that the inferred link between the $G\alpha_s$ and $G\alpha_q$ pathways, uncovered by the genetic screens described herein, is functional rather than developmental.

The hyperactivated $G\alpha_s$ pathway increases neurotransmitter release: Our results suggest that the hyperactive locomotion that occurs upon hyperactivating the $G\alpha_s$ pathway is associated with increased neurotransmitter release. Previous studies have clearly shown that mutations that increase the production of cAMP, as well as application of cAMP or its analogs, can facilitate both nerve-evoked and spontaneous neurotransmitter release (Brunelli *et al.* 1976; Zhong and Wu 1991; Yoshihara *et al.* 1999; Zhang *et al.* 1999). In addition, the often-used method of hypertonicity-induced transmitter release is partially mediated by cAMP (Suzuki *et*

al. 2002). More recently, transgenic activation of $G\alpha_s$ itself in Drosophila was shown to increase basal-evoked transmitter release (Renden and Broadie 2003). The present study does not address how activating the $G\alpha_s$ pathway increases neurotransmitter release; however, previous studies in which cAMP levels and/or protein kinase A activity have been acutely manipulated have demonstrated that the $G\alpha_s$ pathway increases the probability of release (Trudeau *et al.* 1996; Chen and Regehr 1997). A later study found a specific role for cAMP/PKA in recruiting synaptic vesicles from the reserve pool to the readily releasable primed pool (Kuromi and Kidokoro 2000). Applying the insights from these latter studies to our current study leads us to infer that the increased neurotransmitter release and coordinated hyperactive locomotion that results from activating the $G\alpha_s$ pathway in whole animals is a consequence of increased synaptic vesicle priming/probability of release, at least at the specific synapses that drive locomotion.

Presynaptic and postsynaptic roles of the $G\alpha_s$ pathway: Our results show that it is the neuronal, not the muscle, $G\alpha_s$ pathway that mediates the strong suppression of *ric-8(md303)*'s paralysis; however, we could not reproduce the strong levamisole resistance and aldicarb hypersensitivity phenotypes by expressing an *acy-1* gain-of-function transgene solely in muscle or solely in the nervous system, although expression in both tissues using the *acy-1* native promoter did reproduce both phenotypes. This suggests that it is the combined actions of hyperactivating the muscle and nervous system $G\alpha_s$ pathways that leads to strong tolerance to levamisole and hypersensitivity to aldicarb. Previous studies have found that postsynaptic activation of components of the Drosophila $G\alpha_s$ pathway increases neurotransmitter release via retrograde (muscle-to-neuron) signaling (Davis *et al.* 1998; Renden and Broadie 2003). Our finding that aldicarb sensitivity is unaffected by activating the $G\alpha_s$ pathway solely in muscle cells, or solely in neurons, may reflect compensatory mechanisms in which postsynaptic receptor sensitivity, or the composition of the receptor field, is altered in such a way as to prevent us from detecting increased release by our pharmaco-behavioral assays (Davis *et al.* 1998; DiAntonio *et al.* 1999; Renden and Broadie 2003). However, the fact that driving the *acy-1* gain-of-function transgene with its native promoter in both tissues results in signficant drug sensitivity phenotypes is consistent with communication or coordination between the muscle and neuronal $G\alpha_s$ pathways via one or more trans-synaptic signals. Alternatively, it could be that the drug sensitivity phenotypes are dependent on proper expression levels or expression timing factors that are not easily controlled with the ectopic promoters that we used.

In summary, the large forward genetic screens and initial epistasis analysis presented here link RIC-8 (synembryn) and the $G\alpha_s$ pathway with the previously described $G\alpha$-$G\alpha_q$ signaling network. The accompanying study in this issue (Reynolds *et al.* 2005) directly investigates the relationship of the $G\alpha_s$ and $G\alpha_q$ pathways to each other and to synaptic vesicle priming and reveals a role for RIC-8 in maintaining activation of both pathways (Reynolds *et al.* 2005).

The authors are grateful to Bob Barstead and Gary Molder for technical advice that we applied to our SNP mapping method. We also thank Kouichi Iwasaki for providing his *egl-30(tg26)* allele ahead of publication, Ann Rose for providing *unc-13(s69)*, and Celine Moorman and Ron Plasterk for providing *acy-1(pk1279)*. Mike Nonet generously shared information about his ACY-1 (P260S) gain-of-function mutation, isolated independently in his lab and identical to our *acy-1(ce2)*, and also provided a plasmid containing this mutation and helped with our transgene integration protocol. All DNA sequences were obtained from the Core DNA Sequencing Facility at the Oklahoma Medical Research Foundation. Some of the strains used here were provided by the *C. elegans* Genetics Center. This work was supported by a grant from the National Institute of Mental Health to K.G.M. (MH62400).

LITERATURE CITED

Ahnert-Hilger, G., T. Schäfer, K. Spicher, C. Grund, G. Schultz *et al.*, 1994 Detection of G-protein heterotrimers on large dense core and small synaptic vesicles of neuroendocrine and neuronal cells. Eur. J. Cell Biol. **65:** 26–38.

Aravamudan, B., T. Fergestad, W. S. Davis, C. K. Rodesch and K. Broadie, 1999 *Drosophila* Unc-13 is essential for synaptic transmission. Nat. Neurosci. **2** (11): 965–971.

Aronin, N., and M. DiFiglia, 1992 The subcellular localization of the G-protein $G_i\alpha$ in the basal ganglia reveals its potential role in both signal transduction and vesicle trafficking. J. Neurosci. **12** (9): 3435–3444.

Augustin, I., C. Rosenmund, T. C. Südhof and N. Brose, 1999 Munc13–1 is essential for fusion competence of glutamatergic synaptic vesicles. Nature **400:** 457–461.

Bastiani, C. A., S. Gharib, M. I. Simon and P. W. Sternberg, 2003 *Caenorhabditis elegans* $G\alpha_q$ regulates egg-laying behavior via a PLCβ-independent and serotonin-dependent signaling pathway and likely functions both in the nervous system and in muscle. Genetics **165:** 1805–1822.

Berger, A. J., A. C. Hart and J. M. Kaplan, 1998 $G\alpha_s$-induced neurodegeneration in *Caenorhabditis elegans.* J. Neurosci. **18:** 2871–2880.

Betz, A., M. Okamoto, F. Benseler and N. Brose, 1997 Direct interaction of the rat *unc-13* homologue Munc13–1 with the N terminus of syntaxin. J. Biol. Chem. **272** (4): 2520–2526.

Bos, J. L., 1989 ras oncogenes in human cancer: a review. Cancer Res. **49:** 4682–4689.

Bourne, H. R., 1997 How receptors talk to trimeric G proteins. Curr. Opin. Cell Biol. **9:** 134–142.

Brenner, S., 1974 The genetics of *C. elegans.* Genetics **77:** 71–94.

Brundage, L., L. Avery, A. Katz, U. Kim, J. E. Mendel *et al.*, 1996 Mutations in a *C. elegans* $G_q\alpha$ gene disrupt movement, egg laying, and viability. Neuron **16:** 999–1009.

Brunelli, M., V. Castellucci and E. R. Kandel, 1976 Synaptic facilitation and behavioral sensitization in *Aplysia*: possible role of serotonin and cyclic AMP. Science **194:** 1178–1181.

Buechler, Y. J., F. W. Herberg and S. S. Taylor, 1993 Regulation-defective mutants of type I cAMP-dependent protein kinase. J. Biol. Chem. **268:** 16495–16503.

Chase, D. L., G. Patikoglou and M. R. Koelle, 2001 Two RGS proteins that inhibit $G\alpha_o$ and $G\alpha_q$ signaling in *C. elegans* neurons require a Gβ5-like subunit for function. Curr. Biol. **11:** 222–231.

Chen, C., and W. G. Regehr, 1997 The mechanism of cAMP-mediated enhancement at a cerebellar synapse. J. Neurosci. **17:** 8687–8694.

Davis, G. W., A. DiAntonio, S. A. Petersen and C. S. Goodman, 1998 Postsynaptic PKA controls quantal size and reveals a retro-

grade signal that regulates presynaptic transmitter release in *Drosophila*. Neuron **20:** 305–315.

Davis, R. L., J. Cherry, B. Dauwalder, P. L. Han and E. Skoulakis, 1995 The cyclic AMP system and *Drosophila* learning. Mol. Cell. Biochem. **149/150:** 271–278.

DiAntonio, A., S. A. Petersen, M. Heckmann and C. S. Goodman, 1999 Glutamate receptor expression regulates quantal size and quantal content at the *Drosophila* neuromuscular junction. J. Neurosci. **19:** 3023–3032.

Doi, M., and K. Iwasaki, 2002 Regulation of retrograde signaling at neuromuscular junctions by the novel C2 domain protein AEX-1. Neuron **33:** 249–259.

Hajdu-Cronin, Y. M., W. J. Chen, G. Patikoglou, M. R. Koelle and P. W. Sternberg, 1999 Antagonism between $G_o\alpha$ and $G_q\alpha$ in *C. elegans*: the RGS protein EAT-16 is necessary for $G_o\alpha$ signaling and regulates $G_q\alpha$ activity. Genes Dev. **13:** 1780–1793.

Hatley, M. E., B. K. Benton, J. Xu, J. P. Manfredi, A. G. Gillman *et al.*, 2000 Isolation and characterization of constitutively active mutants of mammalian adenylyl cyclase. J. Biol. Chem. **275:** 38626–38632.

Hepler, J. R., and A. G. Gillman, 1992 G proteins. Trends Biochem. Sci. **17:** 383–387.

Hori, T., Y. Takai and T. Takahashi, 1999 Presynaptic mechanism for phorbol ester-induced synaptic potentiation. J. Neurosci. **19:** 7262–7267.

Kamath, R. S., M. Martinez-Campos, P. Zipperlen, A. G. Fraser and J. Ahringer, 2001 Effectiveness of specific RNA-mediated interference through ingested double-stranded RNA in *Caenorhabditis elegans*. Genome Biol. **2:** RESEARCH0002.

Kandel, E. R., 2001 The molecular biology of memory storage: a dialogue between genes and synapses. Science **294:** 1030–1038.

Kandel, E. R., and C. Pittenger, 1999 The past, the future and the biology of memory storage. Philos. Trans. R. Soc. Lond. B Biol. Sci. **354:** 2027–2052.

Klattenhoff, C., M. Montecino, X. Soto, L. Guzman, X. Romo *et al.*, 2003 Human brain synembryn interacts with $G_s\alpha$ and $G_q\alpha$ and is translocated to the plasma membrane in response to isoproterenol and carbachol. J. Cell. Physiol. **195:** 151–157.

Koelle, M. R., and H. R. Horvitz, 1996 EGL-10 regulates G protein signaling in the *C. elegans* nervous system and shares a conserved domain with many mammalian proteins. Cell **84:** 112–125.

Kohn, R. E., J. S. Duerr, J. McManus, A. Duke, T. L. Rakow *et al.*, 2000 Expression of multiple UNC-13 proteins in the *Caenorhabditis elegans* nervous system. Mol. Biol. Cell **11:** 3441–3452.

Korswagen, H. C., J. Park, Y. Ohshima and R. H. Plasterk, 1997 An activating mutation in a *Caenorhabditis elegans* G_s protein induces neural degeneration. Genes Dev. **11:** 1493–1503.

Korswagen, H. C., A. M. van der Linden and R. H. Plasterk, 1998 G protein hyperactivation of the *Caenorhabditis elegans* adenylyl cyclase SGS-1 induces neuronal degeneration. EMBO J. **17:** 5059–5065.

Kuromi, H., and Y. Kidokoro, 2000 Tetanic stimulation recruits vesicles from reserve pool via a cAMP-mediated process in *Drosophila* synapses. Neuron **27:** 133–143.

Lackner, M. R., S. J. Nurrish and J. M. Kaplan, 1999 Facilitation of synaptic transmission by EGL-30 $G_q\alpha$ and EGL-8 PLCβ: DAG binding to UNC-13 is required to stimulate acetylcholine release. Neuron **24:** 335–346.

Landis, C. A., S. B. Masters, A. Spada, A. M. Pace, H. R. Bourne *et al.*, 1989 GTPase inhibiting mutations activate the α chain of G_s and stimulate adenylyl cyclase in human pituitary tumours. Nature **340:** 692–696.

Lin, R. C., and R. H. Scheller, 2000 Mechanisms of synaptic vesicle exocytosis. Annu. Rev. Cell Dev. Biol. **16:** 19–49.

Lyons, J., C. A. Landis, G. Harsh, L. Vallar, K. Grunewald *et al.*, 1990 Two G protein oncogenes in human endocrine tumors. Science **249:** 655–659.

Malenka, R. C., D. V. Madison and R. A. Nicoll, 1986 Potentiation of synaptic transmission in the hippocampus by phorbol esters. Nature **321:** 175–177.

Maruyama, I. N., and S. Brenner, 1991 A phorbol ester/diacylglycerol-binding protein encoded by the *unc-13* gene of *Caenorhabditis elegans*. Proc. Natl. Acad. Sci. USA **88:** 5729–5733.

Mello, C. C., J. M. Kramer, D. Stinchcomb and V. Ambros, 1991 Efficient gene transfer in *C. elegans*: extrachromosomal maintenance and integration of transforming sequences. EMBO J. **10** (12): 3959–3970.

Mendel, J. E., H. C. Korswagen, K. S. Liu, Y. M. Hajdu-Cronin, M. I. Simon *et al.*, 1995 Participation of the protein G_o in multiple aspects of behavior in *C. elegans*. Nature **267:** 1652–1655.

Miller, K. G., and J. B. Rand, 2000 A role for RIC-8 (synembryn) and GOA-1 ($G_o\alpha$) in regulating a subset of centrosome movements during early embryogenesis in *C. elegans*. Genetics **156:** 1649–1660.

Miller, K. G., M. D. Emerson and J. B. Rand, 1999 $G_o\alpha$ and diacylglycerol kinase negatively regulate the $G_q\alpha$ pathway in *C. elegans*. Neuron **24:** 323–333.

Miller, K. G., M. D. Emerson, J. McManus and J. B. Rand, 2000 RIC-8 (synembryn): a novel conserved protein that is required for $G_q\alpha$ signaling in the *C. elegans* nervous system. Neuron **27:** 289–299.

Moorman, C., and R. H. Plasterk, 2002 Functional characterization of the adenylyl cyclase gene *sgs-1* by analysis of a mutational spectrum in *Caenorhabditis elegans*. Genetics **161:** 133–142.

Neer, E. J., 1995 Heterotrimeric G proteins: organizers of transmembrane signals. Cell **80:** 249–257.

Ngsee, J. K., K. Miller, B. Wendland and R. H. Scheller, 1990 Multiple GTP-binding proteins from cholinergic synaptic vesicles. J. Neurosci. **10** (1): 317–322.

Nurrish, S., L. Segalat and J. M. Kaplan, 1999 Serotonin inhibition of synaptic transmission: $G\alpha_o$ decreases the abundance of UNC-13 at release sites. Neuron **24:** 231–242.

Parfitt, K. D., and D. V. Madison, 1993 Phorbol esters enhance synaptic transmission by a presynaptic, calcium-dependent mechanism in rat hippocampus. J. Physiol. **471:** 245–268.

Rand, J. B., and M. L. Nonet, 1997 Synaptic transmission, pp. 611–643 in *C. elegans II*, edited by D. H. Riddle, T. Blumenthal, B. J. Meyer and J. R. Priess. Cold Spring Harbor Laboratory Press, Cold Spring Harbor, NY.

Renden, R. B., and K. Broadie, 2003 Mutation and activation of $G\alpha s$ similarly alters pre- and rostsynaptic mechanisms modulating neurotransmission. J. Neurophysiol. **89:** 2620–2638.

Renger, J. J., A. Ueda, H. L. Atwood, C. K. Govind and C. F. Wu, 2000 Role of cAMP cascade in synaptic stability and plasticity: ultrastructural and physiological analyses of individual synaptic boutons in *Drosophila* memory mutants. J. Neurosci. **20:** 3980–3992.

Reynolds, N. K., M. A. Schade and K. G. Miller, 2005 Convergent, RIC-8-dependent $G\alpha$-signaling pathways in the *Caenorhabditis elegans* synaptic signaling network. Genetics **169:** 651–670.

Richmond, J. E., W. S. Davis and E. M. Jorgensen, 1999 UNC-13 is required for synaptic vesicle fusion in *C. elegans*. Nat. Neurosci. **2** (11): 959–964.

Richmond, J. E., R. M. Weimer and E. M. Jorgensen, 2001 An open form of syntaxin bypasses the requirement for UNC-13 in vesicle priming. Nature **412:** 338–341.

Rizo, J., and T. C. Sudhof, 2002 Snares and Munc18 in synaptic vesicle fusion. Nat. Rev. Neurosci. **3:** 641–653.

Robatzek, M., and J. H. Thomas, 2000 Calcium/calmodulin-dependent protein kinase II regulates *Caenorhabditis elegans* locomotion in concert with a G_o/G_q signaling network. Genetics **156:** 1069–1082.

Robatzek, M., T. Niacaris, K. Steger, L. Avery and J. H. Thomas, 2001 *eat-11* encodes GPB-2, a $G\beta_5$ ortholog that interacts with $G_o\alpha$ and $G_q\alpha$ to regulate *C. elegans* behavior. Curr. Biol. **11:** 288–293.

Sassa, T., S. Harada, H. Ogawa, J. B. Rand, I. N. Maruyama *et al.*, 1999 Regulation of the UNC-18-*Caenorhabditis elegans* syntaxin complex by UNC-13. J. Neurosci. **19:** 4772–4777.

Segalat, L., D. A. Elkes and J. M. Kaplan, 1995 Modulation of serotonin-controlled behaviors by G_o in *Caenhorabditis elegans*. Nature **267:** 1648–1651.

Shenker, A., L. S. Weinstein, A. Moran, O. H. Pescovitz, N. J. Charest *et al.*, 1993 Severe endocrine and nonendocrine manifestations of the McCune-Albright syndrome associated with activating mutations of stimulatory G protein G_s. J. Pediatr. **123:** 509–518.

Singer, W. D., H. A. Brown and P. C. Sternweis, 1997 Regulation of eukaryotic phosphatidylinositol-specific phospholipase C and phospholipase D. Annu. Rev. Biochem. **66:** 475–509.

Sondek, J., D. G. Lambright, J. P. Noel, H. E. Hamm and P. B.

Sigler, 1994 GTPase mechanism of G proteins from the 1.7-A crystal structure of transducin α-GDP-AlF. Nature **372:** 276–279.

Sternweis, P. C., and J. D. Robishaw, 1984 Isolation of two proteins with high affinity for guanine nucleotides from membranes of bovine brain. J. Biol. Chem. **259:** 13806–13813.

Stevens, C. F., and J. M. Sullivan, 1998 Regulation of the readily releasable vesicle pool by protein kinase C. Neuron **21:** 885–893.

Sunahara, R. K., C. W. Dessauer, R. E. Whisnant, C. Kleuss and A. G. Gilman, 1997 Interaction of $G_{s\alpha}$ with the cytosolic domains of mammalian adenylyl cyclase. J. Biol. Chem. **272:** 22265–22271.

Suzuki, K., A. D. Grinnell and Y. Kidokoro, 2002 Hypertonicity-induced transmitter release at *Drosophila* neuromuscular junctions is partly mediated by integrins and cAMP/protein kinase A. J. Physiol. **538:** 103–119.

Tall, G. G., A. M. Krumins and A. G. Gilman, 2003 Mammalian Ric-8A (synembryn) is a heterotrimeric Gα protein guanine nucleotide exchange factor. J. Biol. Chem. **278:** 8356–8362.

Taussig, R., and A. G. Gilman, 1995 Mammalian membrane-bound adenylyl cyclases. J. Biol. Chem. **270:** 1–4.

Tesmer, J. J. G., R. K. Sunahara, A. G. Gillman and S. R. Sprang, 1997 Crystal structure of the catalytic domains of adenylyl cyclase in a complex with $G_{s\alpha}$-GTPγS. Science **278:** 1907–1916.

Timmons, L., D. L. Court and A. Fire, 2001 Ingestion of bacterially expressed dsRNAs can produce specific and potent genetic interference in *Caenorhabditis elegans*. Gene **263:** 103–112.

Trudeau, L. E., D. G. Emery and P. G. Haydon, 1996 Direct modulation of the secretory machinery underlies PKA-dependent synaptic facilitation in hippocampal neurons. Neuron **17:** 789–797.

van der Linden, A. M., F. Simmer, E. Cuppen and R. H. Plasterk, 2001 The G-protein β-subunit GPB-2 in *Caenorhabditis elegans* regulates the $G_o\alpha$-$G_q\alpha$ signaling network through interactions with the regulator of G-protein signaling proteins EGL-10 and EAT-16. Genetics **158:** 221–235.

Van Dop, C., M. Tsubokawa, H. R. Bourne and J. Ramachandran, 1984 Amino acid sequence of retinal transducin at the site ADP-ribosylated by cholera toxin. J. Biol. Chem. **259:** 696–698.

Vetter, I. R., and A. Wittinghofer, 2001 The guanine nucleotide-binding switch in three dimensions. Science **294:** 1299–1304.

Waters, J., and S. J. Smith, 2000 Phorbol esters potentiate evoked and spontaneous release by different presynaptic mechanisms. J. Neurosci. **20:** 7863–7870.

Weimer, R. M., J. E. Richmond, W. S. Davis, G. Hadwiger, M. L. Nonet *et al.*, 2003 Defects in synaptic vesicle docking in *unc-18* mutants. Nat. Neurosci. **6:** 1023–1030.

Wicks, S. R., R. T. Yeh, W. R. Gish, R. H. Waterston and R. H. Plasterk, 2001 Rapid gene mapping in *Caenorhabditis elegans* using a high density polymorphism map. Nat. Genet. **28:** 160–164.

Yoshihara, M., A. Ueda, D. Zhang, D. L. Deitcher, T. L. Schwarz *et al.*, 1999 Selective effects of neuronal-synaptobrevin mutations on transmitter release evoked by sustained versus transient Ca2+ increases and by cAMP. J. Neurosci. **19:** 2432–2441.

Zhang, D., H. Kuromi and Y. Kidokoro, 1999 Activation of metabotropic glutamate receptors enhances synaptic transmission at the *Drosophila* neuromuscular junction. Neuropharmacology **38:** 645–657.

Zhang, G., Y. Liu, A. E. Ruoho and J. H. Hurley, 1997 Structure of the adenylyl cyclase catalytic core. Nature **386:** 247–253.

Zhong, Y., and C. F. Wu, 1991 Altered synaptic plasticity in *Drosophila* memory mutants with a defective cyclic AMP cascade. Science **251:** 198–201.

Zhong, Y., V. Budnik and C. F. Wu, 1992 Synaptic plasticity in *Drosophila* memory and hyperexcitable mutants: role of cAMP cascade. J. Neurosci. **12:** 644–651.

Communicating editor: B. J. Meyer